

**IDENTIFICATION AND DETECTION OF CIS-
PLATIN BINDING PROTEINS BY LASER
INDUCED BREAKDOWN SPECTROSCOPY**

**A Thesis submitted to
the Graduate School of Engineering and Sciences of
İzmir Institute of Technology
in Partial Fulfillment of the Requirements for the Degree of**

MASTER OF SCIENCE

in Chemistry

**by
İbrahim KAYA**

**October 2015
İZMİR**

We approve the thesis of **İbrahim KAYA**

Examining Committee Members:

Prof. Dr. Şerife H. YALÇIN
Department of Chemistry, İzmir Institute of Technology

Prof. Dr. Figen ZİHNİOĞLU
Department of Biochemistry, Ege University

Prof. Dr. Lütü ÖZYÜZER
Department of Physics, İzmir Institute of Technology

26 October 2015

Prof. Dr. Şerife H. YALÇIN
Supervisor, Department of Chemistry,
İzmir Institute of Technology

Prof. Dr. Ahmet Emin EROĞLU
Head of the Department of Chemistry

Prof. Dr. Bilge KARAÇALI
Dean of the Graduate School of
Engineering and Sciences

ACKNOWLEDGEMENTS

I would like to thank to several people who really accompanied and supported me during my thesis studies.

First of all, I am grateful to my thesis supervisor Assoc. Prof. Dr. Şerife H. YALÇIN for her guidance, support and endless knowledge. Her expertise in laser plasma spectroscopy improved my research skills and prepared me for future challenges. I am very grateful to her for giving me the chance of working together.

I am grateful to Assoc. Prof. Dr. Alper ARSLANOĞLU, Prof. Dr. Figen ZİHNİOĞLU, Prof. Dr. Lütfi ÖZYÜZER and Prof. Dr. Şenay BAYSAL, for readily agreed to be my thesis committee members and also for their interest, precious suggestions and spending their valuable time.

Also, I would like to thank to my laboratory mates Semira ÜNAL and Nadir ARAS for their great friendship, help and for the enjoyable times we had together.

I would like to thank to Melda GÜRAY, Ahmet Emin ATİK and Melike DİNÇ from Izmir Institute of Technology Biological Mass Spectrometry and Proteomics Facility Laboratories for helping me in biology laboratory and providing me practical information.

I would like to give my precious thanks to my friends for their help, friendship and support during this thesis period. Thanks for your emotional support and all those great moments that we shared.

Finally, I would like to express my special thanks to my family for their sincere love, support, encouragement and understanding during this study and at every stage of my life. With my deepest gratitude, I dedicate this study to my family.

ABSTRACT

IDENTIFICATION AND DETECTION OF CIS-PLATIN BINDING PROTEINS BY LASER INDUCED BREAKDOWN SPECTROSCOPY

In this study, an all-optically designed laser plasma spectroscopic technique for rapid identification and detection of cisplatin-binding proteins on electrophoretic gel spots prior to molecular mass spectrometric analysis is demonstrated. For this purpose, human serum albumin, human apo transferrin and horse heart myoglobin standard proteins and protein extracts from HeLa cancer cells were subjected to; incubation with cis-platin solution for several hours. Then, non-reducing polyacrylamide gel electrophoretic separation was applied. Followed by the visualization of proteins in the gel by Coomassie Brilliant Blue staining technique protein spots on the gel were dried between two cellophane sheets and subjected to laser ablation by highly energetic laser pulses. In addition, prior to nr-SDS-PAGE separation cis-platin binding to standard proteins were monitored by ESI-MS with several measurements made in 24 hours of incubation time.

Using a Nd:YAG laser at its second harmonic wavelength, 532nm, 10 Hz frequency and 10 ns pulse duration, a micro-plasma was created on dried gel spots. Resulting plasma emission light was collected with collection lenses and transferred to a spectrograph via fiber optic cable. An intensified charge coupled device (ICCD) detector enabled multielemental analysis of platinum binding protein samples. Platinum binding proteins were recognized from the prominent neutral emission line, Pt (I) at 273.3 nm, in a plasma formed by the focused laser pulses on the gel, just in the center or in the vicinity of the electrophoretic spot. Spectral emission intensity of Pt lines from LIBS data has been optimized with respect to laser energy and detector timing parameters. Optimization of LIBS experimental parameters have been studied on polyacrylamide gels soaked in cis-Pt solution for Pt signal.

It has been shown that, LIBS is a suitable method for identifying Pt in proteins, in gel medium, with nanogram levels of detection capability. The technique was applied to HeLa (human cervical cancer cells) cells extract for the detection of Pt-bound HSA after standard addition of known amounts of protein.

ÖZET

SİS-PLATİN BAĞLI PROTEİNLERİN LAZER OLUŞTURMALI PLAZMA SPEKTROSKOPİSİ İLE BELİRLENMESİ VE TAYİNİ

Bu çalışmada, sisplatin bağlı proteinlerin kütle spektrometresi ile analizi öncesinde jel içinde hızlı bir şekilde belirlenmesi ve tayini için tamamen optik tasarıma dayalı bir lazer plazma spektroskopi tekniği gösterilmektedir. Bu amaç için, insan serum albümini, insan apo transferini ve at kalbi miyoglobini standart proteinleri ve HeLa kanser hücrelerinden elde edilmiş protein özütleri sis-platin çözeltisi ile birçok saat inkübe edilmiştir. Daha sonra, indirgeyici olmayan poliakrilamid jel elektroforezi ile ayrılması uygulanmıştır. Proteinler jel içinde Coomassie Brilliant Blue ile görselleştirilmelerinin ardından iki selofan tabakası arasında kurutulup, yüksek enerjili lazer darbeleri ile lazer ablasyonuna tabi tutulmuştur. Buna ek olarak, nr-SDS-PAGE ayırması öncesinde, standart proteinlerin sis-platine bağlanması 24 saat inkübasyon süresinde ESI-MS ile yapılan pek çok ölçüm ile izlenmiştir.

532 nm dalga boyunda, 10 Hz frekansda ışımaya yapan ve 10 ns darbe süreli bir Nd:YAG lazer kaynağı ikinci harmonik dalga boyunda kullanılarak kurutulmuş jel bölgeleri üzerinde mikro plazma oluşturmak için kullanılmıştır. Plazmadan saçılan ışınlar toplama lensleri ile toplanıp fiber optik kablo yardımı ile bir spektrografa transfer edilmiştir. Şiddetlendirilmiş bir CCD detektör sis-platin bağlı proteinleri çoklu element analizini mümkün kılmıştır. Platin bağlı proteinler üzerinde elektroforetik noktanın merkezine veya yakınına odaklanan lazer pulsu ile oluşan plazmada açığa çıkan 273.3 nm deki platinin atomik emisyon çizgisi ile tanımlanır. LIBS datasından elde edilen platinin atomik emisyon çizgilerinin yoğunluğu lazer enerjisi ve detektör zamanlama parametrelerine göre optimize edilmiştir. LIBS'in deneysel parametreleri sis-platin çözeltisinin içine batırılmış polyakrilamid jel üzerinde platin sinyali için çalışılmıştır.

LIBS'in jel ortamındaki proteinlerin platin içeriğini nanogram algılama yeteneği kapasitesiyle araştırılmak için uygun bir yöntem olduğu gösterilmiştir. Teknik HeLa kanser hücreleri ekstraktlarındaki platin bağlı HSA'nın bilinen miktarlarda standart ilave edildikten sonraki tayini için kullanılmıştır.

TABLE OF CONTENT

LIST OF FIGURES	viii
LIST OF ABBREVIATIONS.....	x
CHAPTER 1. INTRODUCTION TO LASER INDUCED BREAKDOWN SPECTROSCOPY (LIBS)..... 1	
1.1. What is Laser Induced Breakdown Spectroscopy (LIBS)	1
1.2. Physics of Laser Ablation and Laser-Induced Plasmas	2
1.2.1. Temperature and Thermodynamic Equilibrium	3
1.2.2. Spectral Lines and Electron Density	3
1.2.3. Temporal Evolution of the Laser-Induced Plasma.....	4
1.3. Advantages and Disadvantages of LIBS.....	6
1.4. LIBS Instrumentation.....	7
1.3.1. Lasers	7
1.3.1.1. Nd:YAG Lasers	8
1.3.2. Optical Materials for LIBS.....	9
1.3.3. Spectrograph and Detection Systems.....	10
1.5. Biological Applications of LIBS	12
CHAPTER 2. METALLODRUG BINDING PROTEINS..... 15	
2.1. Pt-Based Metallodrugs.....	15
2.1.1. Physiology of Cisplatin	17
2.1.2. Interactions of Cisplatin with Proteins	18
2.2. Identification and Detection of Metallodrug Binding Proteins.....	19
2.3. Conventional Analytical Methods for Cisplatin-Binding Proteins.....	20
2.4. Aim of this Thesis and Motivation	22

CHAPTER 3. MATERIALS AND METHODS	24
3.1. Experimental LIBS Set-up.....	24
3.2. Chemicals and Reagents	25
3.3. Methodology	26
3.3.1. Synthesis of Cis-platin Binding Proteins	26
3.3.2. Verification of Cis-platin-Binding to Proteins by ESI-MS	27
3.3.3. nr-SDS-PAGE Separation of Cisplatin Binding Proteins	27
3.3.4. Optimization of Spectral Emission of Pt.....	28
3.4. In Vitro Investigations of Protein Extracts from Cancer Line	29
 CHAPTER 4. RESULTS AND DISCUSSION.....	 30
4.1. Optimization of the Instrumental LIBS parameters.....	30
4.1.1. Effect of Laser Pulse Energy on Signal Intensity	30
4.1.2. Detector Timing Parameters	32
4.2. Verification of Cis-platin-Binding to Proteins by ESI-MS.....	35
4.3. Separation of Cisplatin Binding Protein by nr-SDS-PAGE	41
4.4. Morphology of Laser Ablated Craters on Gel	42
4.5. LIBS Analysis of Cis-platin Binding Proteins in Gel.....	43
4.6. In Vitro Investigations of Protein Extracts from Cancer Line	46
 CHAPTER 5. CONCLUSIONS	 50
 REFERENCES	 51

LIST OF FIGURES

<u>Table</u>	<u>Page</u>
Figure 1.1. Spectral Profiles	4
Figure 1.2. A schematic of the temporal history of a LIBS plasma.	5
Figure 1.3. A schematic representation of a general LIBS apparatus.....	7
Figure 1.4. Nd:YAG laser configuration.	8
Figure 1.5. Schematic of an Echelle Spectrograph.	10
Figure 1.6. A typical diagram of ICCD.	11
Figure 2.1. Molecular structures of the most important Pt-containing drugs.	16
Figure 2.2. Schematic of the uptake and interactions of cisplatin in the cell.	17
Figure 2.3. Molecular Structures of Cysteine and Cystine	18
Figure 3.1. A schematic of the experimental LIBS set-up.....	25
Figure 3.2. BIO-RAD nr-SDS-PAGE set-up.....	28
Figure 4.1. Typical LIBS spectrum of dried polyacrylamide gel soaked in concentrated cis-platin solution (Laser pulse energy: 100mJ, t_d : 1000 ns, t_g :100 μ s, detector gain level: 100, single laser shot).	31
Figure 4.2. LIBS signal intensity variation of Pt (I) lines with respect to laser pulse energy (t_d :1000 ns, t_g :100 μ s).	32
Figure 4.3. LIBS signal intensity variation of Pt (I) at 273.3 nm with respect to detector delay time (Laser pulse energy: 100 mJ, T_g : 100 μ s).	33
Figure 4.4. LIBS signal intensity variation of Pt (I) at 273.3 nm with respect to detector gate time (Laser pulse energy: 100 mJ, T_d : 1000 ns).	34
Figure 4.5. Lateral variation of of Pt (I) lines on the dried polyacrylamide gel samples. Laser pulse energy: 100 mJ, t_d = 2200ns, t_g : 200 μ s. Signals were obtained from 3 consecutive laser shots.	35
Figure 4.6. ESI-MS spectra of myoglobin incubated during 24 h in physiological buffer solution at 37 $^{\circ}$ C.	36
Figure 4.7. ESI-MS spectra of myoglobin incubated with cis-platin solution during 24 h in physiological buffer solution at 37 $^{\circ}$ C.....	37
Figure 4.8. ESI-MS spectra of HSA during 24 h incubation in physiological buffer solution at 37 $^{\circ}$ C.	39

Figure 4.9. ESI-MS spectra of HSA incubated with cis-platin solution during 24 h in physiological buffer solution at 37 °C.	40
Figure 4.10. nr-SDS-PAGE separation of individual standard proteins incubated with cis-platin. The main bands representing the standard proteins are indicated by arrows.	41
Figure 4.11. SEM images of spots after 5 consecutive laser shots on dried polyacrylamide gels in between the hydrophobic membranes (laser pulse energy: 100 mJ, t_d : 2200 ns, t_g : 200 μ s).....	42
Figure 4.12. Representative LIBS spectra of HSA on dried polyacrylamide gels in between the hydrophobic membranes which were obtained from five consecutive laser shots (laser pulse energy: 100 mJ, t_d : 2200 ns, t_g : 200 μ s).	44
Figure 4.13. Qualitative analysis of HSA-Pt, Tf-Pt and Myo-Pt on dried polyacrylamide gels in between hydrophobic membranes after separation (laser pulse energy: 100 mJ, t_d : 2200 ns, t_g : 200 μ s).	45
Figure 4.14. nr-SDS-PAGE and SDS-PAGE patterns of protein extracts from human cervical cancer cells. M: protein molecular weight marker.	46
Figure 4.15. nr-SDS-PAGE gel showing separation of protein extracts from human cervical cancer cells and HSA incubated with cisplatin, along with the protein molecular weight markers (M). HSA-Pt complex indicated by arrow. Bands showing the polymerization of HSA indicated in circles.	47
Figure 4.16. Representative LIBS spectra of HSA-Pt complex and protein extracts (laser pulse energy: 100 mJ, t_d : 2200 ns, t_g : 200 μ s).	48
Figure 4.17. nr-SDS-PAGE gel showing separation of protein extracts added HSA. M: molecular weight marker, C: protein extract without HSA, and 1,2,3 represents concentration gradient of protein extracts added HSA. HSA-Pt complexes indicated by arrows.	49

LIST OF ABBREVIATIONS

AAS	atomic absorption spectroscopy
CCD	charged coupled device
DNA	deoxyribonucleic acid
ESI-MS	electrospray ionization mass spectrometry
ESI-Q-TOF	electrospray ionization-quadrupole-time of flight
FOCs	fiber optic cables
GSH	glutathione
HPLC	high performance liquid chromatography
HSA	human serum albumin
ICCD	Intensified charge coupled device
LASER	light amplified stimulated emission of radiation
LA-ICP-MS	laser ablation inductively coupled plasma mass spectrometry
LIBS	laser-induced breakdown spectroscopy
LTE	local thermodynamic equilibrium
MALDI-MS	matrix assisted laser desorption ionization mass spectrometry
MCP	microchannel plate
MYO	myoglobin
mJ	millijoule
MT	metallothionein
Nd	neodymium
nanosecond	nanosecond
PCA	principal component analysis
PC	photocathode
Pt	platinum
SDS-PAGE	sodium dodecylsulfate polyacrylamide gel electrophoresis
TF	transferrin
TLC	thin layer chromatography
t_g	detector gate time
t_d	detector delay time
YAG	yttrium aluminum garnet
μ s	microsecond

CHAPTER 1

INTRODUCTION TO LASER INDUCED BREAKDOWN SPECTROSCOPY (LIBS)

1.1. What is Laser Induced Breakdown Spectroscopy (LIBS)

Laser-Induced Breakdown Spectroscopy, LIBS also called as Laser Induced Plasma Spectroscopy, (LIPS) and Laser Ablation Spectroscopy, (LAS) is an optical atomic emission spectrochemical technique that has experienced an important increase in the number of applications in the past few decades after Cremers and Radziemski's first experiment on the detection of beryllium on filters using a laser plasma (Cremers and Radziemski 1985).

The technique uses an intense pulsed laser beam to investigate the multielemental composition of a sample by creation of a high-temperature micro plasma which is followed by time-resolved optical spectroscopic analysis. After laser ablation and evolution of laser plasma, some part of the emitted light is collected by a fiber-optic cable and the light emitted by atomic and ionic species is dispersed by a spectrometer. Then, the recording of the emission signals are performed by a detector and electronics display the results after digitizing.

Recently, different approaches have been performed to improve the signal intensities in LIBS experiments. Double-pulse LIBS (De Giacomo et al. 2005), resonance-enhanced LIBS (Chan and Cheung 2000) and laser-induced fluorescence detection of elements in laser plasma (LIBS-LIF) (Laville et al. 2009) are the most significant signal enhancement techniques of LIBS.

Laser-induced plasma is typically weakly ionized plasma which consists of mixture of atoms, ions and free electrons and is overall electrically neutral. Ideally, the LIBS technique intends to obtain optically thin plasma in which a thermodynamic equilibrium exists and represents the elemental composition of the target sample.

During the last few decades the potential of LIBS technique has experienced a big growth and it has been used for several areas of analytical chemistry including: civilian and military applications (DeLucia Jr et al. 2005) environmental (Capitelli et al. 2002) and geochemical analysis (Harmon et al. 2006), Cultural heritage (Gaona et al.

2013), archeological science (Giakoumaki, Melessanaki, and Anglos 2007), space applications (Sallé et al. 2005), analysis of pharmaceuticals (St-Onge et al. 2002), biomedical applications (Diedrich, Rehse, and Palchaudhuri 2007) and many others. Recently, it has been proved that LIBS is a promising, sensitive and specific technique for cancer research by detecting cancer biomarkers in blood plasma (Markushin et al. 2015).

1.2. Physics of Laser Ablation and Laser-Induced Plasmas

The LIBS process includes laser interaction with the target material, removal of sample mass (ablation), plasma formation (breakdown), expansion and element specific ionic/atomic emission lines and decay. Detection of element specific ionic/atomic emission lines are employed during expansion and decay stages of the plasma (Cremers et al. 2006).

Laser material interaction is initiated by absorption of laser energy by the sample from a pulsed radiation field. The pulse durations are generally on the order of nanoseconds, however pico- and femto-second laser pulses have been used for LIBS. When the temperature goes up the boiling point of the sample material, absorbed energy converted into heating, ending with vaporization of the sample which is called ablation. Formation of a vapor above the sample surface is observed after removal of a tiny amount of particulate matter from the surface. Then the laser pulse starts heating the resulting vapor plume. The vapor condenses into droplets which are only few micrometers causing absorption and scattering of laser radiation which results in ionization, strong heating and plasma formation. Resulting plasma undergoes a fast expansion and subsequent cooling. Spectroscopic atomic and ionic emission lines may can be observed one microsecond after the pulse which leads ablation (Russo, Mao, and Mao 2002).

Electron temperature, electron density and thermodynamic equilibrium are the key concepts to explain the physics of laser-induced plasmas.

1.2.1. Temperature and Thermodynamic Equilibrium

To describe laser-induced plasma, the combination of electrons, atoms, molecules and ions should be characterized. Plasma properties can be characterized by a single temperature, if there is a complete thermodynamic equilibrium. However, since thermodynamic equilibrium is not complete in every region of the plasma, a useful approximation, local thermodynamic equilibrium (LTE) has been proposed (Griem 1963). According to LTE, thermodynamic equilibrium exists in a small part of the plasma, even though it can be different in every part. To be able to think through the concept of LTE, enough number of collisions should be occurred to heat the plasma and diffuse the energy to all the regions and species.

Electron temperature, pressure, electron density, relative population of energy levels and distribution of velocity of plasma species can be explained through the concept of a single temperature, when a local thermodynamic equilibrium exists. Therefore, LTE is a crucial concept for a quantitative analysis in laser-induced plasmas.

1.2.2. Spectral Lines and Electron Density

Electron density and plasma temperature are important parameters related to the widths and intensities of spectral lines. Shifting and broadening in the line shapes can be used to diagnose the broadening mechanism.

For low plasma densities, Doppler broadening and natural broadening determines the linear shape of the spectral lines. Doppler broadening is due to the thermal motions of the emitting particles which can be resulted in either red- or blue-shifting, whereas natural broadening is a result of Heisenberg's uncertainty principle. For high plasma densities, spectral line shapes are dominated by Stark effect which is due to the strong electrical fields caused by fast- and slow-moving electrons in the plasma. Splitting and shifting in the atomic and ionic energy levels causes broadening of the spectral lines as a result of Stark effect (Griem 2005).

Another broadening mechanism is collision broadening which is a result of the collisions with neutral particles.

Figure 1.1. represents the spectral line profiles of a LIBS spectrum. Gaussian line profiles are a result of pure Doppler broadening, whereas Lorentz profiles are

natural line broadening and collision broadening. Voigt profiles results from the convolution of Gaussian and Lorentz profiles. Γ represents the full-width at half maximum.

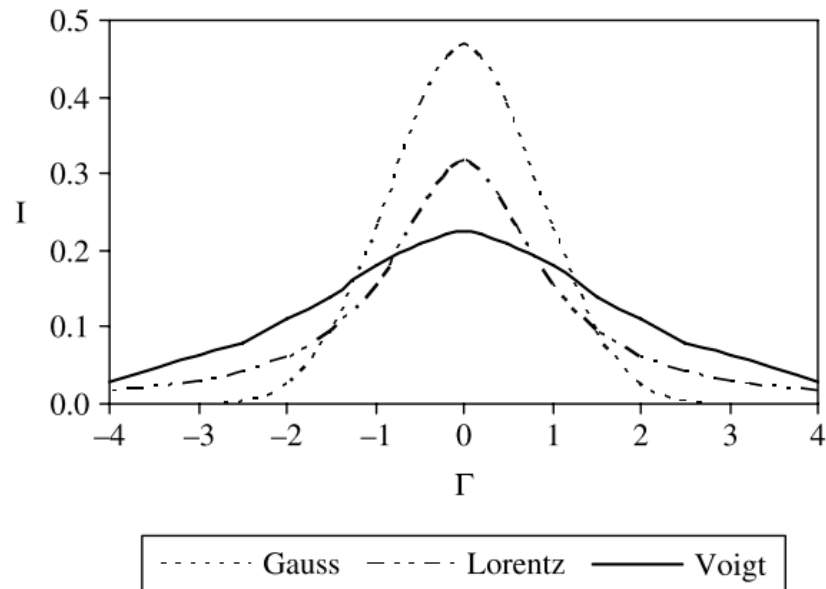


Figure 1.1. Spectral Profiles
(Source: Cremers et al. 2006)

Normally, Doppler and Stark effects are the most significant contributors to the line widths. The Doppler width can only be related to the atomic mass and temperature of the species, whereas Stark effect mostly results from collision of the emitting species with electrons rather than ions. Therefore, electron densities can be calculated using the lines broadened by Stark effect (Griem 2005).

1.2.3. Temporal Evolution of the Laser-Induced Plasma

Most of the LIBS experiments have been performed by nanosecond-duration laser pulses beside some applications of picosecond- and femtosecond-duration laser pulses (Singh and Thakur 2007).

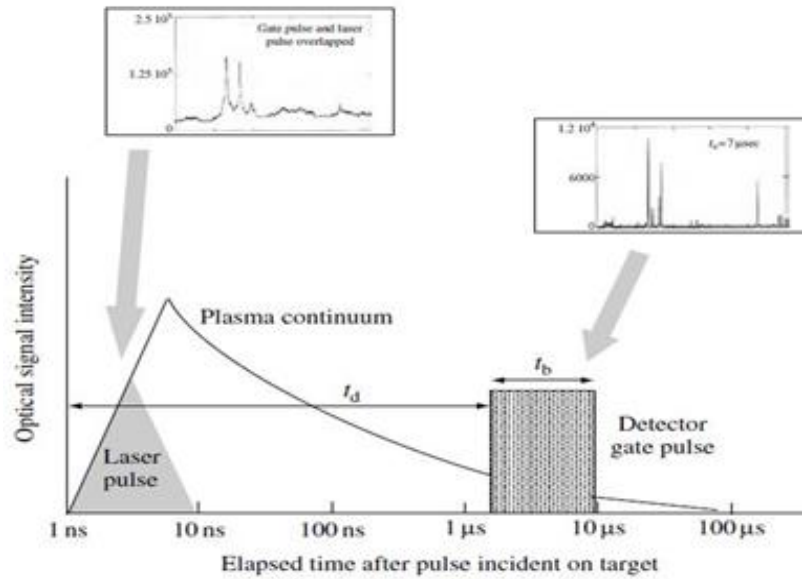


Figure.1.2. A schematic of the temporal history of a LIBS plasma (Source: Cremers et al. 2006)

Figure 1.1 shows the temporal history of a LIBS plasma initiated by a single ten nanosecond-duration laser pulse. At early times of the plasma there is a background plasma continuum which is mainly due to bremsstrahlung and recombination radiations. Bremsstrahlung occurs during the acceleration or deceleration of the electrons during collisions in the plasma. In recombination event, excess kinetic energy of an electron is given up in the form of radiation (photon) after a free electron trapped into an ionic or atomic energy level in the plasma. The background continuum radiation decays faster than the elemental spectral lines which hinders the ability of detection (Miziolek, Palleschi, and Schechter 2006). Thanks to the time resolution of the plasma light, analysis of the time interval according to the signals of interest is possible during LIBS experiments.

The time between the beginning of the laser pulse to the opening of the detector gate is represented by the symbol t_d which is called delay time. And the length of time in which the detector gate is open is represented by the symbol t_g which is called detector gate time. During the measurements ionic spectral lines are observed at early times of the plasma after background radiation. As the electrons starts to recombine with ions neutral atoms, and then the molecules form. Laser energy, t_d , and t_g are the key parameters which should be optimized according to the signal of interest during LIBS studies.

1.3. Advantages and Disadvantages of LIBS

Operational simplicity, versatility and relatively low cost are some of the features of LIBS that make it superior over the other atomic emission spectroscopic techniques. Multi-elemental analysis of solid, liquid and gas samples is possible with simultaneous detection of all elements present in the sample. Before LIBS analysis there is little or no sample preparation stages required which prevents possible contamination of the analyte.

LIBS is a non-destructive method since laser pulse ablates only a tiny amount of sample. A micrometer range of spatial and depth resolution is possible for surface analysis.

Remote analysis of samples is possible with LIBS using fiber optic cables to transport laser pulse to the sample and to collect emitted light from the plasma. This feature makes LIBS a good in-situ analysis technique (Cremers, Barefield, and Koskelo 1995).

Beside several advantages, LIBS has some disadvantages to be considered. During surface analysis, since plasma is formed on a very tiny micrometers size area, the spectral emission after laser ablation may not always represent the actual concentrations of species in the bulk solid samples. Composition of the surface may differ from the bulk of the sample which can cause an error in the result of analysis.

LIBS has a relatively poor accuracy beside its low precision due to the shot to shot variations and fluctuation in laser energy. LIBS has relatively poor sensitivity and detection limits (sub-ppm and high-ppb concentrations) compared to the other atomic emission spectroscopic techniques. However, recent signal enhancement techniques have been successfully performed to improve the detection limits by several orders of magnitude for analytes in aqueous solutions (Wang et al. 2015).

Geometric position of the sample's surface with respect to laser pulse is one of the key factors that affect the results during the analysis of the solid samples. A deflected focusing of the laser beam on to the target material can change the ablated mass of the sample and therefore plasma parameters like electron temperature, electron density and the intensity of the emitted light may vary (Singh and Thakur 2007).

1.4. LIBS Instrumentation

A typical experimental LIBS set-up, schematically shown in Figure 1.1, contains three main parts. A high energy pulsed laser source pulse to create a luminous plasma, and optics to direct, focus, reflect and collect the incident laser beam and the light emitted from the plasma, and a spectrograph equipped with a time resolved detector for spectrochemical analysis.

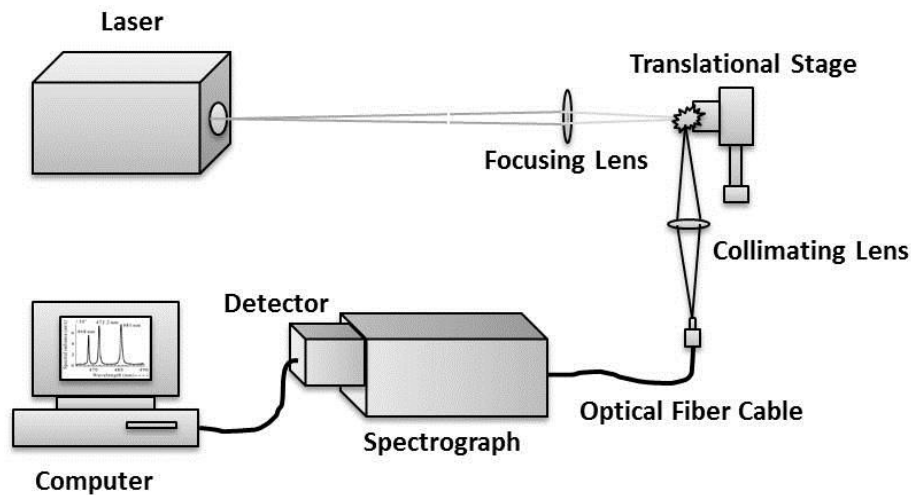


Figure 1.3. A schematic representation of a general LIBS apparatus.

The system additionally contains a laser head, detector gating and control electronics, and a computer control for digitizing and data acquisition. Depending on the samples physical state (solid, liquid, gas), different sample introduction components or equipments may involved.

1.3.1. Lasers

A laser is a device which can produce coherent, monochromatic, and well collimated intense beam of light. Comparing with the other sources of light, lasers are extremely pure monochromatic radiation. The photons making up the laser light are all in a fixed phase relationship (coherence) with respect to each other and a laser light has a very low divergence. Thanks to these properties, lasers are used in a wide variety of

applications in every part of life. The term laser stands for (L)ight (A)mplification by (S)timulated (E)mission of (R)adiation.

There are several types of lasers according to their pump source and gain medium and can be listed as dye lasers, gas lasers, semiconductor lasers and solid state lasers. Flashlamp-pumped Nd:YAG solid state laser system which is used for most of the LIBS experiments will be discussed in detail.

1.3.1.1. Nd:YAG Lasers

Flashlamp-pumped solid state Nd:YAG lasers are mostly preferred laser types for LIBS experiments. Nd:YAG lasers have high power densities which are needed to form a plasma when focused to a small spot, and high repetition rates which can be used for dual-pulse LIBS experiments. It is feasible to obtain a megawatt power levels with Nd:YAG lasers with a suitable optical configuration. In addition, Nd:YAG laser systems are easy to operate, and does not require very skillful technical person.

Nd:YAG lasers are a classical four-level laser systems in which more efficient emission of radiation is provided with a smaller pumping energy. Most of the Nd:YAG laser systems are operated at its fundamental wavelength of 1064 nm. However, it is possible to use second, third and fourth harmonic wavelengths at 532 nm, 355 nm and 266 nm respectively, using nonlinear frequency conversion crystals (Bordui and Fejer 1993).

Figure 1.3. shows a typical flashlamp-pumped Nd:YAG laser configuration. This laser system consists of flashlamps (F) which can be from near UV to near IR spectral regions, a laser rod (LR) which is doped with Nd (Neodymium) ions in a Yttrium Aluminum Garnet (YAG) crystal matrix, two reflective mirrors (M) one is partially transmitting, and a Q-switch shutter (Q) to provide powerful laser pulses.

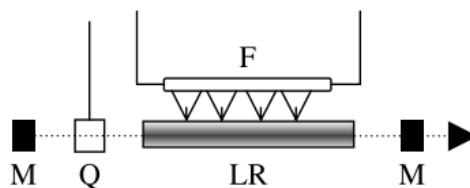


Figure 1.4. Nd:YAG laser configuration
(Source: Cremers et al. 2006)

Briefly, little part of the pumping light which is provided by flashlamps absorbed by Neodymium (Nd) ions in lasing medium. Thanks to the energy levels of Nd ions in the lasing medium, if pumping from flashlamp is strong enough, a population inversion is succeeded in which the number of electrons on the upper transition level of the electronic energy levels are more than the number of electrons in terminating electronic energy level. After population inversion, a photon which has the same frequency as the lasing transition will establish stimulated emission in which some of the ions will decay to the lower state of the energy levels. Therefore, the photon will result in increased gain or amplification. Amplification of the light at the lasing wavelength will be provided because of the reflected amplified light back into the laser rod (Kiss and Pressley 1966).

Powerful lasers pulses which are needed to form a micro LIBS plasma are achieved by using pulsed and Q-switched lasers. Q switch shutter is used to prevent the photons completing a full path in the lasing medium which directs the photons back into the lasing medium causing stimulated emission and increasing the population inversion rate. When Q-switch becomes transparent with time gated laser pulse, high power laser pulses can be obtained in short duration times. Typical duration times of the pulses for Nd:YAG lasers with Q-switch mode are 5-10 ns. Partially transmitting mirror allows the passage of a part of the pulse from the cavity (Miziolek, Palleschi, and Schechter 2006).

1.3.2. Optical Materials for LIBS

Lenses or mirrors are used to focus the laser pulses on to the target material. They are also used to collect the emission light from the laser-induced plasma. Due to the dependence of the optical materials on wavelength, focal position of a lens system depends on the wavelength of the laser beam. This feature shows differences according to the construction material of the lenses. For example, focal length of the lens will increase with increased wavelength of the laser light for quartz materials (Singh and Thakur 2007).

To minimize the energy lose for the optical systems, anti-reflection coatings are used to remove back reflections and reflections from the optics which will maximize the energy focused on a target.

For an Nd:YAG laser spherical optics are used to provide a radially symmetric laser beam. Lens types (plano convex, double convex, etc.) are important for LIBS

applications. The most appropriate lenses should be chosen to obtain the least deflection from the radially symmetric focusing on the target.

Fiber optic cables (FOCs) are also widely used optical materials in LIBS systems due to their ability to transmit the light by a total internal reflection. Emitted light from the laser induced plasma can be collected and carried with high efficiency with FOCs. For remote analysis LIBS systems FOCs are used to transfer the plasma light from remote distances (Cremers, Barefield, and Koskelo 1995).

1.3.3. Spectrograph and Detection Systems

Most of the LIBS systems use a spectrograph which is connected to a CCD array. Recently, echelle type spectrographs have been the most preferred spectrographs because of their longer wavelength range (UV-NIR) compared to Czerny-Turner design spectrographs.

The light is dispersed in two orthogonal directions by echelle spectrograph. The result is 2D patterned data which can be combined with a 2D detector such as ICCD.

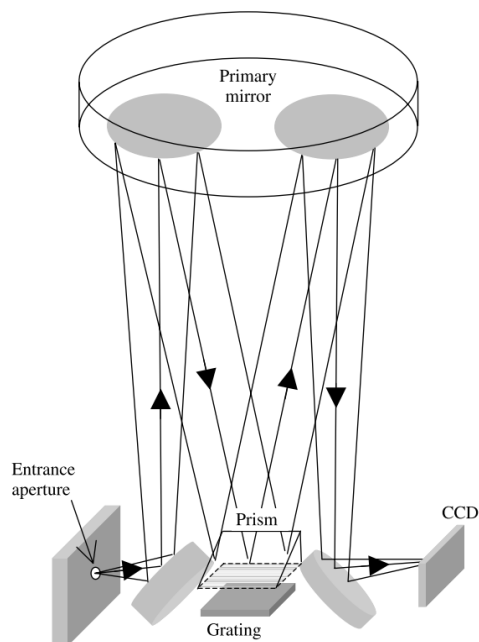


Figure 1.5. Schematic of an Echelle Spectrograph
(Source: Cremers et al. 2006)

As shown in Figure 1.4 echelle type spectrographs provides a very dispersed spectra because of the fact that they are used at a high angle. However, only a short interval of wavelength is dispersed in every grating. Another dispersing element such as

prism is used to separate overlapped different orders of grating. Then, CCD detectors can detect these separate orders of grating thanks to their two-dimensional detection ability.

Figure 1.5 shows a schematic of an ICCD detector which contains three main parts; a photocathode (PC), a microchannel plate (MCP) and phosphor screen. CCD is connected to a MCP to provide time-gate detection of the laser-induced plasma. With the help of a high voltage applied, photons hit the surface of photocathode and ejected electrons travels in MCP producing many electrons because of multiple reflections. When the multiplied electrons strike the phosphor screen, they are transferred to the CCD camera via fiber optic taper to be intensified (Miziolek, Palleschi, and Schechter 2006).

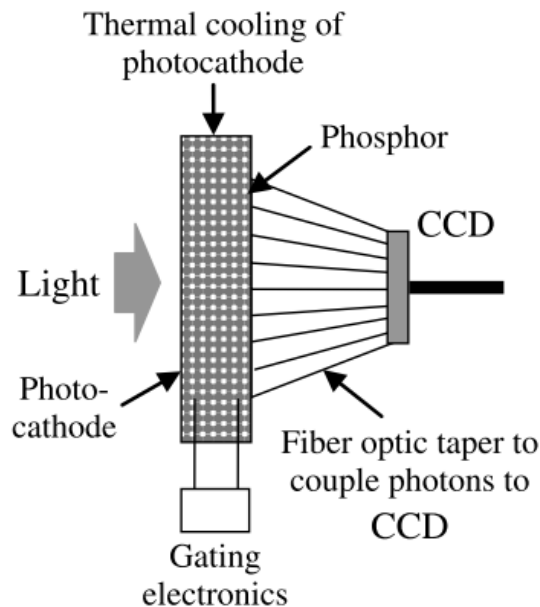


Figure 1.6. A typical diagram of ICCD
(Source: Cremers et al. 2006)

For LIBS systems, intensified CCD detectors are the most widely used detection systems thanks to their ability to make two dimensional spatial analysis and to perform simultaneous multi-elemental analysis with a timed resolved detection. ICCD is also capable of reaching a time-resolved detection of few nanoseconds.

1.5. Biological Applications of LIBS

Recent developments in laser-induced breakdown spectroscopy (LIBS) turned LIBS into a very useful tool which can be used for the analysis of complex biological materials and clinical samples without using any reagent. LIBS has been used to analyze several human clinical specimens such as teeth (Singh, Kumar, and Sharma 2014), bones (Samek et al. 2001), tissue sections (Kumar et al. 2004), blood (Markushin et al. 2015) and other fluid samples beside microorganisms (e.g. moulds, bacteria, yeasts) (Samuels et al. 2003) that can have an influence on human health. The capability of LIBS to make sensitive multi-elemental analysis, rapidly detect trace elements at low concentrations (sub-ppm concentrations), easily perform remote analysis, and sensitively analyze and characterize several kinds of biological and clinical samples has recently increased the number of publications with high impact factors demonstrating the advances in LIBS technology.

High sensitivity to all of the elements in the periodic table and compatibility with advanced chemometric methods makes LIBS a useful tool to be used for quick identification and discrimination of any unknown material. Samuels et al. 2003 have studied discrimination of bacterial pollens, molds, spores and proteins using the chemometric method called principal component analysis (PCA). With increasing signal intensities with multiple fiber optic cables, it has been shown that LIBS is capable of distinguishing bacterial pollens, spores and molds. Another interesting study was performed by Rehse, Diedrich, and Palchoudhuri 2007. They investigated the discrimination and identification of *Pseudomonas aeruginosa* bacteria grown in bile and blood to diagnose some diseases. They determined the content of some inorganic elements by LIBS and used discriminant function analysis (DFA) to discriminate different types of bacteria. A recent research was performed by Manzoor et al. 2014 in which 40 bacterial strains have been identified and classified according to the small changes in their atomic composition resulted by their mutations or genetic variations. Laser-induced breakdown spectroscopy combined with a chemometric method called neural networks (NN) has been used to identify bacterial strains causing hospital acquired infections.

LIBS has been used to perform trace element analysis of different parts of human and animal body. Sun et al. 2000 demonstrated that LIBS can be used to perform trace elements analysis in human skin. They detected Zn content in human stratum

corneum with an exponential decrease with depth in the skin. Samek et al. 2001 investigated the potential of LIBS for calcified tissue analysis. They performed the multi-dimensional analysis of trace elements Al, Sr, and Pb in bone and teeth samples. Their results were consistent with the results of atomic absorption spectroscopy (AAS). Another application of LIBS to dentistry was performed by Singh and Rai 2011. They detected the varying amounts of trace elements in healthy teeth and caries and explained their role in the formation of caries. Haruna et al. 2000 demonstrated the use of LIBS for the detection of Ca in human hair and nails with high sensitivity. They discussed the capability of their method to monitor the daily intake of Ca and to screen osteoporosis. Yueh et al. 2009 investigated the capacity of LIBS for the discrimination and identification of organ and tissue types. They performed LIBS analysis on brain, lung, spleen, liver, kidney tissue samples and demonstrated that LIBS can discriminate between tissues and can help with the identification of the organ and tissue type. Recently, Sancey et al. 2014 investigated the multi-elemental imaging and quantification of biological tissues with the LIBS technique combined with optical microscopy. They demonstrated 10 μm resolution and ppm-level detection level on murine kidneys. Quantification of metallic elements Gd, Na, Fe and Si was succeeded in the tissue with a good sensitivity which is in the range of tens of attomoles per laser pulse.

Kumar et al. 2004 performed the first experiments to investigate the capability of using LIBS as a tool to be used for cancer research. They tried to discriminate malignant tissue from normal tissue. They reported that the ratio of the elements Ca/K and Cu/K are significantly different from each other. Therefore, they concluded that LIBS has a potential to be used as an *in vivo* tool for cancer diagnosis. Another interesting study for cancer diagnosis was performed by El-Hussein et al. 2010. They proclaimed that discrimination of cancerous tissue from a normal tissue can be done comparing their Ca and Mg amounts. Increasing the sensitivity under vacuum conditions (10^{-2} torr), they concluded that Mg and Ca intensities are higher in cancerous tissue than normal tissue. They also discussed that increasing Ca signal intensities in cancerous tissues can be attributed to the fact that people with cancer usually have hypercalcemia. A recent study was performed by Markushin et al. 2015. They used femtosecond laser-induced breakdown spectroscopy to detect biomarker cancer antigen 125 (CA125) in human blood plasma. Their approach was tagging the biomarker with magnetic nanoparticles and performing multielemental analysis by LIBS. With

femtosecond LIBS they obtained highly sensitive results. They concluded that their method can be used to detect and monitor cancer biomarkers in human blood plasma with a high sensitivity.

Aside from human and animal tissue samples, LIBS is also used to analyze plant tissue samples. Samek et al. 2006 used femto second laser-induced breakdown spectroscopy to perform the chemical analysis of leaf samples. With the acquired LIBS spectra, they have reported the spatial distribution of Fe within the leaf. They discussed that their technique can be a tool to identify the storage and monitoring of iron ions in different compartments of the leaf samples. Another study was performed by Kaiser et al. 2009. They performed the mapping analysis of Pb, Mg and Cu elements within the leaves of sunflower. LA-ICP-MS and LIBS techniques were complementarily used. Their resolution was up to 200 μm in cm^2 area of the leaves of sunflower. The results were compared with the results from atomic absorption spectroscopy (AAS) and thin layer chromatography (TLC). As a result, it is shown that LA-ICP-MS and LIBS can replace AAS when a fast elemental mapping is needed. A recent study performed by Aras and Yalçın 2014. They developed a novel LIBS method for rapid identification and detection of the phosphorus content of proteins in SDS gel spots after electrophoretic separation. The technique was utilized to identify the phosphorus signals of electrophoretically separated proteins of canola plant extract with a nanogram level detection limit.

LIBS can be a useful tool to be applied for astrobiological applications thanks to its ability to perform remote analysis. Although LIBS is known to be appropriate for inorganic identification, recent advances allow LIBS to identify and discriminate organic biological samples. Therefore, LIBS is used on Mars Science Laboratory. Summons et al. 2011 have been working on the applications of LIBS for exobiology. They have been evaluating the effect of different atmospheres on the biological identification and discrimination. They also reported that LIBS can be used to analyze elemental composition of any surface on Mars up to seven meters away from the Mars Rover.

In this thesis study, identification and detection of Pt-binding proteins by LIBS was investigated. Platinum content of cis-platin binding standard proteins and proteins of extracts from HeLa cells (human cervical cancer cells) were investigated by LIBS after separation by nr-SDS-PAGE. The technique was successfully applied to standard proteins and HSA-added protein extracts with a nano gram limit of detection.

CHAPTER 2

METALLODRUG BINDING PROTEINS

Advances in the knowledge of coordination and redox properties of metal ions have stimulated a big interest in the development and applications of metal-based drugs in medicine for decades. After the success of cisplatin as an anti-tumor drug, many other metal complexes have been used clinically. For example, gold complexes have been used against rheumatoid arthritis (Sutton et al. 1972), bismuth complexes successfully applied as antiulcer drugs (McColm et al. 1996), compounds with Ga, Ru, Rh, As, and Sn have shown antitumor properties (Sun, Tsang, and Sun 2009) and platinum compounds have been successfully used against cancer (Wong and Giandomenico 1999).

Detection and identification of the target biomolecules and understanding the molecular mechanisms of physiology of these metal-based compounds are crucial to understand their side effects and mechanism of resistance.

2.1. Pt-Based Metallodrugs

Pt containing drugs cisplatin, carboplatin, and oxaliplatin are the most efficient metallodrugs which have been used worldwide for clinical purposes. Rosenberg, Van Camp, and Krigas 1965 firstly reported the antitumor properties of cisplatin (cis-diaminedichloro-platinum(II)). As a result of interaction with DNA nucleobases, cisplatin damages the structure of DNA, disrupts many cellular processes and induces cell death. However, due to the interactions of cisplatin with other biomolecules, several toxic side effects including neurotoxicity and nephrotoxicity are observed (Pinto and Lippard 1985).

To minimize cisplatin's side effects, many other Pt-based drugs have been synthesized and their clinical applications have been performed. Carboplatin (cis-diamine (1,1-cyclobutanedicarboxylato)platinum(II)) represents a lower reactivity and toxicity when compared to cisplatin. As a second generation drug, carboplatin is widely used against ovarian and lung cancer (Jodrell et al. 1992). A third generation drug oxaliplatin ((trans-RR-cyclohexane-1,2-diamine)oxalatoplatinum(II)) shows higher

toxicity than cisplatin and it is highly effective against colon cancer (Tesniere et al. 2010). Figure 2.1. shows the molecular structures of some important Pt-containing metallodrugs. Especially, satraplatin (JM216) has been studied in detail and it is used against prostate cancer (Adis and Profile 2007). Nedaplatin, lobaplatin, and picoplatin are the other promising drugs which are used against small-cell lung cancer (Wong and Giandomenico 1999).

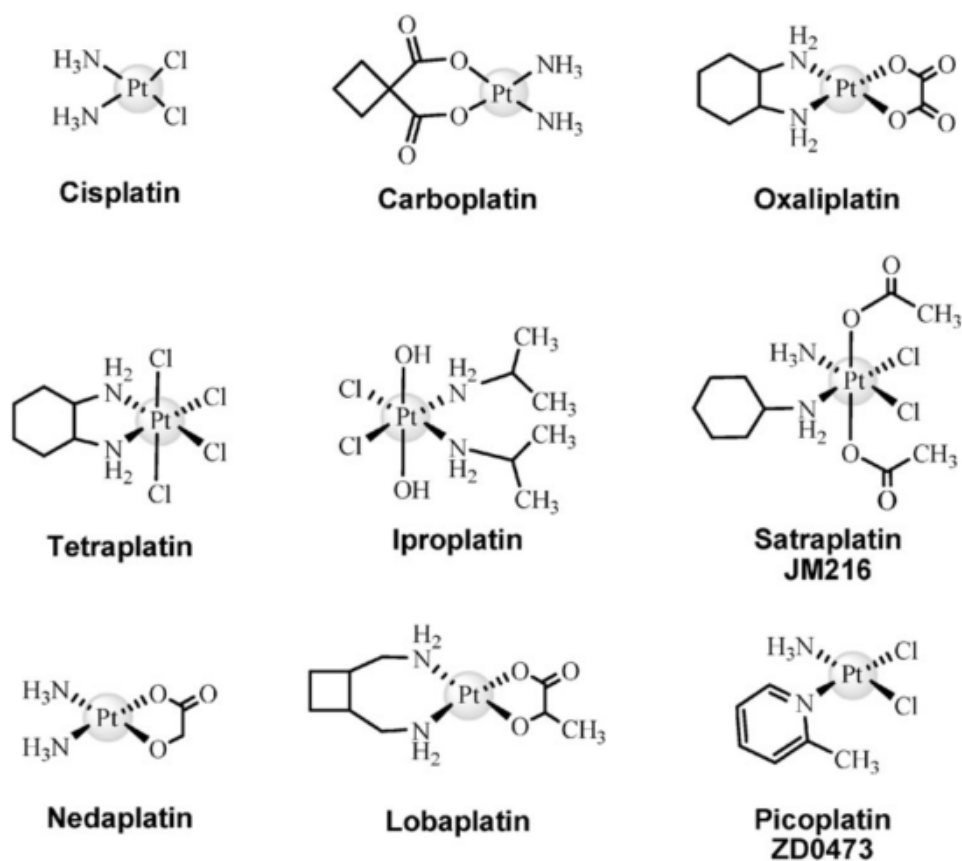


Figure 2.1. Molecular structures of the most important Pt-containing drugs
(Source: Esteban-Fernández et al. 2010)

Determination of molecular mechanisms and elucidation of intermediate metabolites of Pt-containing drugs are crucial to understand the physiological role and functions of these metal complexes. With the improvement of the analytical tools and methods in the last few decades, there has been a great increase in the number of studies involving the drug interaction mechanisms of carboplatin, oxaliplatin and cisplatin. The most widely used antitumor Pt-based drug for analytical chemistry research is cisplatin and its mechanism of interactions with biomolecules will be reviewed in detail, below.

2.1.1. Physiology of Cisplatin

Since it is injected to the patients intravenously, interactions of cisplatin with biological molecules (e.g nucleic acids, proteins, lipids and other macromolecules) will determine the physiological effects like anticancer efficiency, toxicity, cellular uptake, transport and accumulation (Timerbaev et al. 2006).

Different chemical conformations of cisplatin are often observed when it is interacting with the target biomolecule. According to the aqueous medium, different hydrolyzed forms of cisplatin can form (Cui and Mester 2003), which may show different reactivity with biomolecules in the cell and blood stream. Although it is possible to observe dimers and diaqua species of cisplatin in aqueous solution, there is no evidence of their existence at room temperature. The most abundant hydrolysed form of cisplatin is its monoaqua form which is inhibited by high NaCl content (Kondo et al. 1996).

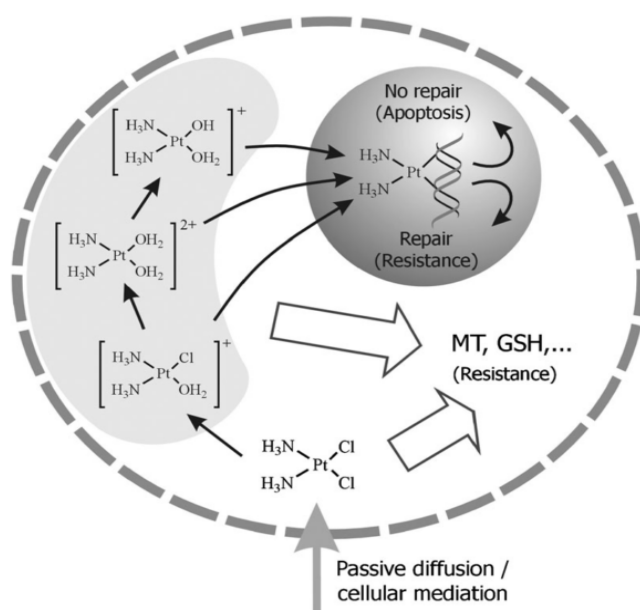


Figure 2.2. Schematic of the uptake and interactions of cisplatin in the cell (Source: Esteban-Fernández et al. 2010)

The entrance and interactions of cisplatin in the cell is schematically shown in Figure 2.2. Cisplatin enters the cell as a neutral molecule mostly in a passive diffusion way. Once cisplatin diffused into the cytoplasm of the cell, hydrolysis of cisplatin is forced due to the low concentration of chloride ion in the cytosol. After hydrolysis, different conformations of cisplatin can interact with the DNA nucleobases disrupting

their structure and inducing cellular death via apoptosis. However, many other biological molecules such as MT (metallothioneins), GSH (glutathione), lipids, peptides and proteins may react with cisplatin and lead to detoxification and resistance effects.

Effectivity of cisplatin depends on several factors including, interactions of cisplatin with membrane proteins of the cell (Allardyce et al. 2001), saline concentration of cytosol (Kondo et al. 1996), interactions of cisplatin with biomolecules other than DNA and fate of evolving adducts after cisplatin's interactions with target molecules (Timerbaev et al. 2004).

2.1.2. Interactions of Cisplatin with Proteins

Pt(II) behaves as a soft Lewis acid. Therefore, it shows a high affinity for S-donor, N-donor and O-donors which are soft bases. As a result, aside from DNA nucleobases, other nucleophiles such as blood peptides and proteins which contains S- and N-containing aminoacids are the potential targets of cisplatin (Timerbaev et al. 2006).

Figure 2.3 shows molecular structures of cysteine and cystine molecules. Cystines are aminoacids formed by the oxidation of two cysteine molecules covalently linked by a disulfide bond. Since cystines have S-donors, they have affinity to bind to Lewis acids. Therefore, cystines play important roles in the formation of three-dimensional structure of proteins.

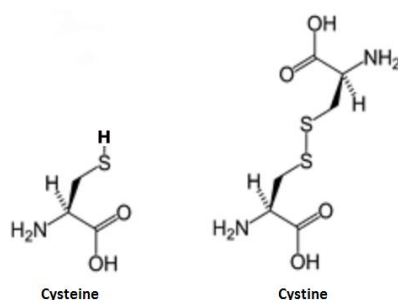


Figure 2.3. Molecular Structures of Cysteine and Cystine

When cisplatin binds to the cystines of proteins, it is possible that it may change the conformation, structure and biological function of the proteins. Therefore, it is highly significant to investigate the interactions of cisplatin with proteins.

Human serum albumin (HSA) and transferrin (Tf) are important blood proteins which can have substantial roles in cisplatin's physiology. HSA is the most abundant blood protein with a concentration of 40-45 g per liter. It has several crucial physiological functions including control of osmotic pressure and transport, metabolism, distribution of many important molecules such as metallodrugs. One mole of HSA can bind up to 10 moles of cisplatin within 50 h incubation (Timerbaev et al. 2004). Efficient binding of cisplatin to HSA can be explained by the fact that cisplatin has a high affinity to sulfur-containing regions which are cysteine residues in the structure of HSA. Transferrins are the key proteins that control the free iron level in biological fluids. Tf is found in human plasma with a concentration of 2.5 g per liter. It is reported that one mole of Tf can bind up to 5.9 moles of cisplatin within 96 h incubation (Moreno-Gordaliza et al. 2012).

Myoglobin (MYO) is also a protein which is widely used for the cisplatin-protein interaction studies. It is an iron- and oxygen-binding protein which is found in muscle tissue of vertebrates. It is reported that one mole of MYO can bind up to 1.3 moles of cisplatin within 96 h incubation (Moreno-Gordaliza et al. 2012).

2.2. Identification and Detection of Metallodrug Binding Proteins

Due to the low concentrations and complexity of the metallodrug-protein adducts, molecular and atomic mass spectrometry techniques combined with a high resolution separation technique are required for the analysis of metallodrug interactions with proteins.

Before their determination, liquid chromatography or electrophoretic techniques are used to separate or isolate the drug-biomolecule adducts for bio-speciation analysis. Most of the chromatographic techniques are coupled with inductively coupled plasma mass spectrometry (ICP-MS) or electrospray ionization mass spectrometry (ESI-MS) due to their high sensitivity and compatibility.

Aside from liquid chromatographic separation techniques, polyacrylamide gel electrophoresis (PAGE) is a technique which provides high-resolution separation of protein-drug adducts according to their net charge, charge/mass ratio and molecular shape in an applied electrical field. It has been reported in a number of researches that certain metallodrug-protein bonds are affected by the reducing conditions during electrophoretic separation (Raab et al. 2009). Denaturing chemicals used in sodium

dodecyl sulfate polyacrylamide gel electrophoresis (SDS-PAGE) can result in metallodrug-protein bond losses causing changes in their native conformations (Mena et al. 2011). Therefore, non-reducing sodium dodecyl sulfate polyacrylamide gel electrophoresis (nr-SDS-PAGE) in which the structure of protein-drug adduct is protected seems to be an appropriate technique for the separation of protein-metallodrug complexes. Details and procedures of nr-SDS-PAGE employed in this thesis study is given in Part 3.3.3.

For identification of drug-protein adducts, soft ionization sources such as matrix-assisted laser desorption/ionization (MALDI) and electrospray ionization (ESI) are used because of the fact that they can ionize large molecules with a minimum change in their unity. ESI is a soft ionization technique which is used for the evolution of gas phase-multiply-charged ions of thermally sensitive large macromolecules without fragmentation. Since ESI-MS provides a softer ionization process and is simply combined with several separation techniques, it is a more preferred technique than MALDI-MS for studying the structure of metallodrug-protein adducts.

In conclusion, to investigate interactions of a metallodrug with proteins, proper separation techniques should be chosen in order to preserve the integrity of adducts. Then, they should be either combined or complementarily used with an atomic or molecular detection technique.

In this study, LIBS detection of Pt content in cisplatin binding proteins were performed in dry gel spots after nr-SDS-PAGE separation. ESI-MS has been used to verify cisplatin binding to standard proteins.

2.3. Conventional Analytical Methods for Cisplatin-Binding Proteins

In the past decades identification and quantification of Pt content in biological samples has been extensively studied using several analytical methodologies like adsorptive voltammetry (Nygren et al. 1990) and atomic absorption spectroscopy (Pera and Harder 1977). Recently, the most preferred analytical technique is ICP-MS due to its high sensitivity. Esteban-Fernandez et al. 2008 reported 63 ng L^{-1} limit of detection for Pt of in cytosolic samples.

Esteban-Fernández et al. 2008 has studied the interactions of cisplatin with serum proteins with atomic HPLC-ICP-MS and ESI-Q-TOF molecular mass spectrometry techniques. They have investigated the interactions of standard proteins

albumin, transferrin, and immunoglobulin G and serum samples with cisplatin. It is reported that albumin is more efficiently binding to cisplatin than transferrin does after analysis of serum samples by HPLC-ICP-MS. Physiological levels of the two proteins were 3 mg L^{-1} for apo-Tf and 30 mg L^{-1} for HSA and total complexation for HSA was 24 h but in the case of apo-Tf only 50% of the protein was complexed after 96 h.

Mena group investigated the optimum conditions for the separation of platinum-binding proteins (Mena et al. 2011). After polyacrylamide gel electrophoretic separation, gel spots were mineralized before acidic digestion and analyzed with ICP-MS to detect platinum content. They concluded that non-reducing conditions are appropriate to preserve the integrity of platinum-protein adduct during gel electrophoresis. Different amounts of proteins in the range of 0.3-2.0 μg were loaded in the gel and analyzed. Detection limits from one gel were 10.1 pg, 10.3 pg, 2.4 pg for Tf-cisplatin, for HSA-cisplatin and for MYO-cisplatin, respectively.

In another research, Moreno-Gordaliza et al. 2012 studied the cisplatin-protein complexes with LA-ICP-MS after two dimensional gel electrophoresis. Cisplatin treated rat serum samples were separated by two dimensional gel electrophoresis. After drying and transferring to nitrocellulose membranes, gels were analyzed by LA-ICP-MS. Pt signals detected on some protein spots including albumin, transferrin and apolipoprotein. Experiments with standard protein samples of equine heart cytochrome c, human serum transferrin, human serum albumin, carbonic anhydrase and horse heart myoglobin indicated that increasing molecular weight of the protein increases the platinum-protein binding ratio which is due to the more nucleophilic sides on bigger proteins available. Moreover, human serum transferrin and human serum albumin has shown nearly the same efficiency of binding with cisplatin. An experimental limit of detection was shown by dropping an amount of 2.5 pg of a Pt solution on a 7 mm^2 surface of nitrocellulose membrane.

Prior to mass spectrometric analysis like ES-MS and MALDI-MS, pre-concentration methods such as solvent evaporation, freeze-drying, ultra filtration are required due to the low concentration levels of Pt-protein adducts in most of the samples. Pt-protein adducts deformation, protein denaturation and sample losses are possible results in pre-concentration stages. Moreover, ESI-MS and MALDI-MS are not compatible with high saline content of the samples which occurs after pre-concentration. Tryptic digestion used for converting proteins into smaller peptides is also another common procedure in proteomics research which may results with losses in

Pt-protein binding and post-translational modifications prior to mass spectrometric analysis (Shevchenko et al. 2006).

2.4. Aim of this Thesis and Motivation

Pt-binding protein analysis mostly performed by highly sensitive mass spectrometric techniques due to the low concentrations of analytes in real samples. However, pre-concentration and sample preparation procedures and acidic digestion before mass spectrometric analysis can always result in contamination or losses of the metal-protein binding. Although, mass spectrometric techniques can provide a high performance, complexity of the required equipments prevents them from being a routinely applied practical method to be used in research laboratories. LIBS is a simple, rapid and sensitive optical spectroscopic technique which requires no sample preparation. Therefore, LIBS is a promising analytical tool for the identification of Pt-binding proteins on electrophoretic gel spots prior to molecular mass spectrometric analysis.

This research aims to investigate the limitations and capabilities of laser-induced breakdown spectroscopy for in-gel identification and detection of cisplatin-binding to physiologically important proteins prior to mass spectrometric analysis for proteome research. For this purpose, human serum albumin, human apo transferrin and horse heart myoglobin standard proteins and protein extracts from HeLa cancer cells were subjected to; incubation with cis-platin solution for several hours. Then, non-reducing polyacrylamide gel electrophoretic separation was applied. Followed by the visualization of proteins in the gel by Coomassie blue staining technique (Chrambach et al. 1967), protein spots on the gel were dried between two cellophane sheets and subjected to laser ablation by highly energetic laser pulses. In addition, prior to nr-SDS-PAGE separation cis-platin binding to standard proteins were monitored by ESI-MS with several measurements made in 24 hours of incubation time.

Using a Nd:YAG laser at its second harmonic wavelength, 532 nm, 10 Hz frequency and 10 ns pulse duration, a micro-plasma was created on dried gel spots. Resulting plasma emission light was collected with collection lenses and transferred to a spectrograph via fiber optic cable. An intensified charge coupled device (ICCD) detector enabled multielemental analysis of platinum binding protein samples.

Spectrochemical analysis of the luminous plasma produced by the focused laser pulses on stained gel spots reveals information about the elemental content and the presence of platinum in a specific protein spot. Gel spots identified by LIBS for their platinum content are then further analyzed by MS for structural identification after in-gel digestion and extraction procedures were applied.

Platinum binding proteins were recognized from their prominent neutral emission line, Pt (I) at 273.3 nm, in a plasma formed by the focused laser pulses on the gel, just in the center or in the vicinity of the electrophoretic spot. Spectral emission intensity of Pt lines from LIBS data has been optimized with respect to laser energy and detector timing parameters. Optimization of LIBS experimental parameters have been studied on polyacrylamide gels soaked in cis-Pt solution for Pt signal.

In this study, an all-optically designed laser plasma spectroscopic technique for rapid identification and detection of cisplatin-binding proteins on electrophoretic gel spots prior to molecular mass spectrometric analysis is demonstrated. From the standard protein solutions (60 μ M) incubated with cis-platin solution (2.4 mM), LIBS emission signals were observed for Pt-HSA and Pt-Apo-transferrin complex however, no signal from the Pt-Myo complex has been observed. It has been shown that, LIBS is a suitable method for identifying Pt in proteins, in gel medium, with ng-pg levels of detection capability. The technique was utilized to identify the Pt signals in HSA-Pt complex after electrophoretically separated proteins from HSA-added HeLa cells (human cervical cancer cells) extract with a nanogram level detection limit.

CHAPTER 3

MATERIALS AND METHODS

In this thesis study, a LIBS experimental set-up was designed and assembled from its commercial components to determine the platinum content in dried nr-SDS PAGE gel spots. A polyacrylamide gel soaked in cis-platin solution was used to optimize spectral emission of LIBS Pt lines with respect to laser energy and detector timing parameters; t_d (delay time) and t_g (gate time). Standard proteins and protein extracts from HeLa cells (human cervical cancer cells) were subjected to; first incubation with cis-platin solution for several hours and second non-reducing polyacrylamide gel electrophoretic separations. Verification of cis-platin binding to standard proteins have been performed by ESI-MS measurements prior to nr-SDS-PAGE separation. After electrophoretic separation, proteins were stained by Coomassie Brilliant Blue staining technique and destained. LIBS experiments have been performed on dried gels under optimum experimental conditions.

3.1. Experimental LIBS Set-up

An experimental LIBS system have been assembled from its commercial components. A schematic of the LIBS set-up used in this work has been shown in Figure 3.1. The LIBS system is consisted of; a laser source, focusing and collection optics, a detection unit, a xyz-translational stage and a video camera system. A Q-switched flash-lamp pumped Nd:YAG laser source (Quanta-Ray Lab-170, Spectra Physics, California-USA) has been operated at its second harmonic, 532 nm. Pulse duration and repetition rate of the laser beam was 10 ns and 10 Hz, respectively. 532 nm reflective mirrors (1" OD, coated, 532 nm reflective, New Focus, Darmstad-Germany) were used to direct the laser beam onto the sample. Focusing the laser beam onto the sample surface have been performed by 17,5 cm focal-length plano-convex lens. Pulse energy of laser beam was measured by a power meter (PE50BB-DIF-V2, Nova II, Ophir, Israel).

Sample was mounted on XYZ-translational stage (New Focus, Darmstad-Germany) to provide fresh spots on the sample surface for each laser pulse. Plasma

emission light is collected and focused onto the core of a fiber-optic cable (Ocean Optics, QP450-2-XSR, 455 μm diameter) by two plano-convex lenses of 20 cm and 10 cm focal lengths. This fiber-optic cable is used to carry plasma emission light onto the entrance slit of the echelle spectrograph (Mechelle 5000, Andor Inc., f/7) combined with an intensified charged coupled device (ICCD) (iStar DH734, Andor Inc.). The spectrograph and detection system spectral range is between 200-850 nm with 0.08 nm resolution at 400 nm. Hg-Ar spectral calibration lamp was used for wavelength calibration of the echelle spectrograph and a black and white video camera system (Honeywell HMM9, Louisville, KY, 40299, USA) was used to view protein spots on the gel for ablation.

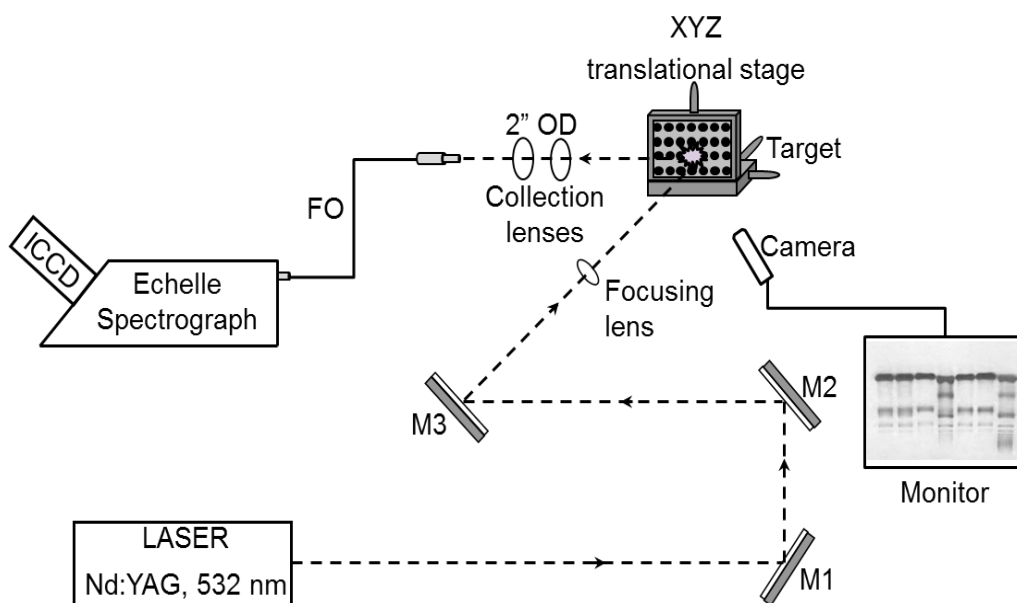


Figure 3.1. A schematic of the experimental LIBS set-up.

3.2. Chemicals and Reagents

The platinum-based drug cisplatin, human serum albumin (HSA), human apo-transferrin (TF) and myoglobin from equine heart (MYO) were also purchased from Sigma-Aldrich (Sigma-Aldrich Chemie, St.Louis, MO). Sodium chloride (Sigma-Aldrich), 2-amino-2-hydroxymethyl-1,3-propanediol Tris (Applichem) and high-purity HCl (Merck) were used to prepare buffer solution for incubation under physiological conditions. HPLC grade organic solvents methanol, ethanol and formic acid used in ESI-MS experiments were purchased from Sigma-Aldrich.

Acrylamide / bis (30% T, 2,67% C Stock), Tris-HCl (1.5 M , pH:8.8 and 0.5M, pH:6.8), 10% ammonium persulfate (Applichem) and tetramethylethylenediamine (Applichem) solutions were used for nr-SDS-PAGE experiments. Ammonium persulfate solutions were prepared freshly before each experiment due to its instability at room temperature even if protected from light or air. Protein solutions and unstained protein molecular weight marker (SM0431, Fermentas) were prepared for once then kept under -20 °C temperature for future uses. Coomassie Brilliant Blue (Applichem) staining solutions were prepared once and used throughout the subsequent experiments. Destaining solution (25% methanol and 75% dH₂O) was prepared freshly for each new experiment.

For extraction of total protein content from human cervical cancer cells (HeLa cells) a mammalian cell lysis reagent (Fermentas, K0301, ProteoJET™) in the presence of protease inhibitor cocktail (cOmplete™, Mini, EDTA-free, Roche) was used.

All the aqueous solutions prepared with ultrapure water (Milli-Q, Millipore, USA).

3.3. Methodology

3.3.1. Synthesis of Cis-platin Binding Proteins

To mimic the intracellular physiological saline and pH conditions, human apo-transferrin (Sigma-Aldrich T1147), human serum albumin (Sigma-Aldrich A3782) and myoglobin from equine heart (Sigma-Aldrich M1882) (60 μM) were separately incubated with cis-platin solution (2400 μM) at a molar ratio 1:40 in a buffer solution containing NaCl (4.64 mM) and Tris-NO₃ (10 mM, pH 7.4). Then, the solutions were incubated for 96 h at 37 °C in a thermostatic bath (JP Selecta 7471200). Control samples were also prepared by incubating the same proteins under the same conditions without cisplatin solution. For the purpose of removing unreacted cisplatin and small molecular weight components of the mixture, sample solutions were subjected to filtration with 3 kDa cut-off filters (Amicon Ultra-0.5 mL Ultracel-3, Millipore) by centrifugation at 14,000 × g for 32 minutes. Then the filter was reversed and the fraction containing cisplatin-bound proteins was collected at 1000 × g for 3 minutes. The filtrate then was diluted with ultrapure water and kept under -20 °C for future experiments.

3.3.2. Verification of Cis-platin-Binding to Proteins by ESI-MS

Solutions of HSA, apo-Tf and MYO were prepared with and without cisplatin as already described above. All the solutions were diluted to 5 μ M concentration and cisplatin binding to proteins were monitored via ESI-MS during 24 h.

All mass spectrometry experiments were conducted on a LTQ XL linear ion-trap mass spectrometer (Thermo Finnigan, San Jose, CA, USA) equipped with an electrospray ionization (ESI) source. The system was operated in the positive mode and the spray voltage was set to + 5.0 kV and the heated capillary temperature adjusted at 300 °C. 5 μ M protein solutions were introduced into the ion source with an incorporated syringe pump at a flow rate of 5 μ L per minute. The protein working solutions were prepared in MeOH/ dH₂O/ HCOOH (50:50:1, v/v/v) containing mixture. Nitrogen was used as a sheath, an auxiliary, and a sweep gas with flow rates of 10, 1, 1 (in arbitrary unit), respectively. Full scan MS spectra were acquired in the m/z range of 150-2000 and scans obtained in 2 minutes were averaged in profile mode.

3.3.3. nr-SDS-PAGE Separation of Cisplatin Binding Proteins

Cis-platin bound proteins were electrophoretically separated by nr-SDS-PAGE before identification and detection of their platinum content by LIBS. nr-SDS-PAGE separation technique was performed according to Laemmli SDS-Polyacrylamide Gel Electrophoresis procedure (Laemmli 1970) without using denaturing reagents such as 2-mercaptoethanol (2-ME) and sodium dodecyl sulfate (SDS). BIO-RAD SDS-PAGE apparatus shown in Figure 3.2 was used for the experiments. Resolving and stacking gels were prepared with monomer concentrations of 12% and 4%, respectively. Finally, 10-40 μ L of samples were loaded into the wells of the gel and then 60 V and 100 V of voltage was applied for 0.5 h and 2h, respectively.



Figure 3.2. BIO-RAD nr-SDS-PAGE set-up.

After running the gel electrophoretic separation of cisplatin-bound proteins, the gel was removed from BIO-RAD SDS-PAGE apparatus and stained with a Coomassie Black Blue staining solution (50% methanol, 10 % acetic acid, 0.05% Coomassie Brilliant Blue R250 and 40% dH₂O) by shaking at 15 rpm speed for overnight. After this step, the gel was placed into a destaining solution (25% methanol and 75% dH₂O) for about 3 h until the protein spots become visible. Finally, this gel was mounted in between two hydrophobic membranes (Gel air Drying System, Bio-RadTM) and left for drying at room temperature prior to LIBS analysis.

3.3.4. Optimization of Spectral Emission of Pt

A resolving gel (monomer concentration 12%) was prepared without using SDS and placed into a concentrated cisplatin solution (6 mM) to soak the gel in cisplatin. After shaking at 30 rpm speed for about 12h, this resolving gel was left for drying on a flat surface at room temperature. In order to determine the optimum experimental parameters for Pt (I) signal intensity at 273.396 nm, LIBS experiments have been performed on the dried gel with an ICCD detector gain level of 100. Optimum laser energy and detector timing parameters; t_d (delay time) and t_g (gate width) were determined according to the spectral emission lines of Pt (I) in LIBS data. Subsequent experiments were carried out at optimum laser energy of 100 mJ and detector timing parameters; delay time of 2200 ns and gate width of 200 μ s where maximum Pt (I) line emission was observed.

3.4. In Vitro Investigations of Protein Extracts from Cancer Line

Total proteins from human cervical cancer cells (HeLa cells) were extracted using a mammalian cell lysis reagent (Fermentas, K0301, ProteoJET™) in the presence of protease inhibitor cocktail (cOmplete™, Mini, EDTA-free, Roche).

Total protein concentrations of extract solutions were determined by Quick Start Bradford protein assay (Bio-Rad Laboratories, Inc., Hercules, CA, USA). Seven different concentrations of bovine serum albumin (BSA): 2, 1.5, 1, 0.75, 0.5, 0.25, 0.125, 0.025 mg/L were used as standard solutions for quantification. Standard and sample solutions were mixed with 30× Bradford reagent, vortexed and incubated for 10 minutes. The assay was performed in 96-Well Microplates (UV-Star®, Greiner Bio-One) and absorbance was measured at 595 nm in an HP8453 UV-visible spectrophotometer (Agilent Technologies Inc., Waldbronn, Germany). The resulting linear range for BSA determination by Bradford protein assay is between 125-1000 µg/L, and total protein concentration of the extract was determined as 600 µg/L.

Protein extract solutions were incubated with a concentrated cis-platin solution at a molar ratio 1:40 in a buffer solution containing NaCl (4.64mM) and Tris-NO₃ (10 mM, pH 7.4) to mimic physiological conditions. Then, the solutions were incubated for 24 h at 37 °C in a thermostatic bath (JP Selecta 7471200). Control samples were also prepared by incubating the total protein extract under the same experimental conditions without cis-platin solution. For pre-concentration of the sample and removal of possible unreacted cis-platin, the mixtures were ultra-filtrated using 10 kDa cut-off filters (Amicon Ultra-0.5 mL Ultracel-3, Millipore).

nr-SDS-PAGE separation of incubated solutions were carried out with the same procedure as described already before in section 3.3.1, using a larger gel apparatus to improve the resolution of the separation. Stained protein spots on dried gels in between the hydrophobic membranes were subjected to subsequent laser shots to determine their platinum content and were then further analyzed by MS for structural identification after in-gel digestion and extraction procedures were applied.

CHAPTER 4

RESULTS AND DISCUSSION

In this thesis study, a LIBS experimental set-up was designed and assembled from its commercial components to determine the platinum content in dried nr-SDS PAGE gel spots. Standard proteins and protein extracts from HeLa cells (human cervical cancer cells) were subjected to; first incubation with cis-platin solution for several hours and second non-reducing polyacrylamide gel electrophoretic separation. Verification of cis-platin binding to standard proteins have been performed by ESI-MS prior to nr-SDS-PAGE separation. After electrophoretic separation, proteins were stained by Coomassie Brilliant Blue staining technique and destained. LIBS experiments have been performed on dried gels under optimum experimental conditions.

4.1. Optimization of the Instrumental LIBS parameters

A polyacrylamide gel soaked in a concentrated cis-platin solution (6mM) was used to optimize spectral emission of Pt lines at 273.3 nm with respect to laser energy and detector timing parameters; t_d (delay time) and t_g (gate time).

4.1.1. Effect of Laser Pulse Energy on Signal Intensity

In LIBS experiments, laser pulse energy is a crucial instrumental parameter affecting ablation processes and plasma formation. Energy per unit area is a more important parameter than the absolute value of laser pulse energy for laser-matter interactions. Therefore, irradiance (energy per unit area and time, W cm^{-2}) and fluence (energy per unit area, J cm^{-2}) are energy-related terms primarily used in LIBS measurements. When the laser fluence is only sufficient to create a plasma plume, the laser pulse rapidly heats, melts and vaporizes the solid material just above the surface. Then, a part of the laser pulse energy heats the evaporated solid material. While the plasma is weakly ionized, ionic and atomic elemental signals are observed with a high background noise in the spectra which results in low sensitivity. At high laser fluences,

the surface is shielded due to the opacity of the plasma resulting non-stoichiometric ablation of analyte from the target surface. Therefore, for LIBS experiments laser pulse energy should be optimized for analyte emission signal with a high signal to noise (S/N) ratio.

All optimization experiments were carried out under the same focusing distance (17.5cm), spot size (100 μm) and a constant laser pulse duration time (10 ns). Therefore, experiments were performed to optimize the absolute value of laser pulse energy.

Figure 4.1 shows a representative LIBS spectrum of dried polyacrylamide gel soaked in a concentrated cis-platin solution. Pt (I) emission line at 273.3 nm was optimized with respect to laser pulse energy.

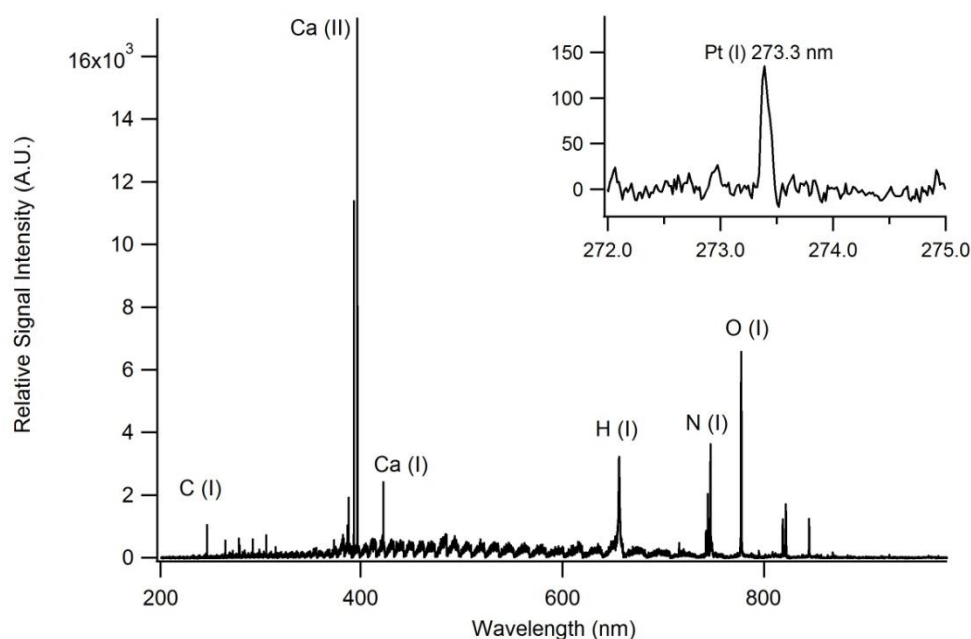


Figure 4.1. Typical LIBS spectrum of dried polyacrylamide gel soaked in concentrated cis-platin solution (Laser pulse energy: 100 mJ, t_d : 1000 ns, t_g : 100 μs , detector gain level: 100, single laser shot).

Figure 4.2. shows LIBS signal intensity variation of Pt (I) lines with respect to laser pulse energy at 273.3 nm emission wavelength from dried polyacrylamide gel samples. Each data was obtained from 5 consecutive laser shots from the same spot. Linear increase in signal intensity observed up to 90 mJ laser pulse energy, whereas a drastic decrease was observed after 110 mJ due to the cracking of the dried gel surface with high laser pulse energies (This part will be supported by SEM pictures, in part xx).

Therefore, 100 mJ was chosen as the optimum laser pulse energy for future experiments to obtain the highest signal intensity.

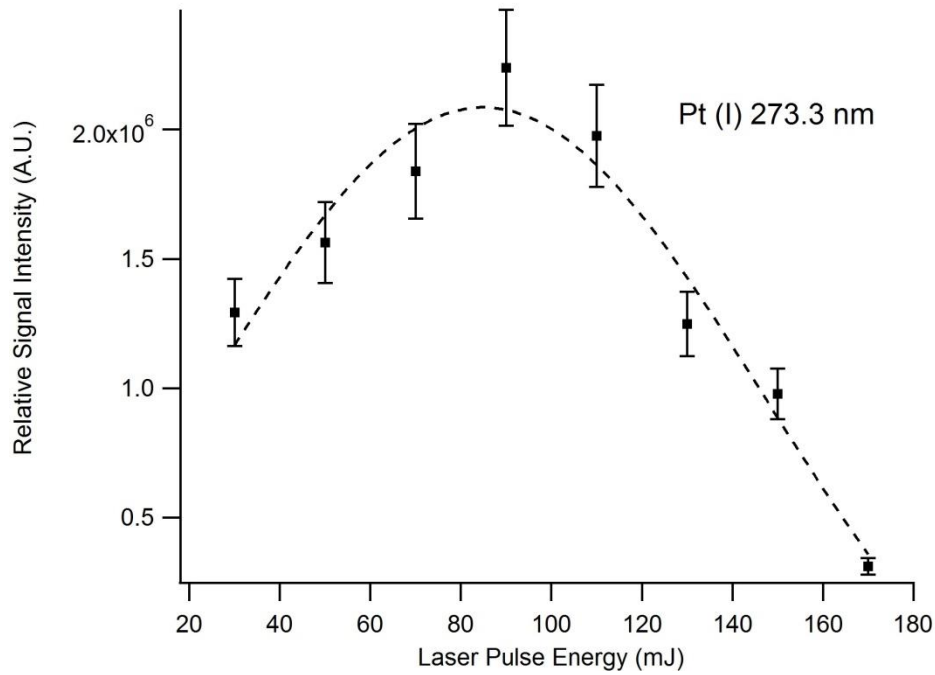


Figure 4.2. LIBS signal intensity variation of Pt (I) lines with respect to laser pulse energy (t_d :1000 ns, t_g :100 μ s).

Energy optimization experiments have been performed at fixed detector timing parameters; delay time and gate time. A constant delay time of 1000 ns and gate time of 100 μ s were used with a detector gain level of 100.

4.1.2. Detector Timing Parameters

Early times of the laser-induced plasma is dominated by a background continuum emission. The decay time of this continuum radiation depends on several factors, such as laser wavelength, energy and pulse duration time, ambient pressure and sample features. Therefore, optimal time window in terms of acquisition time and delay time should be determined case by case to obtain strong line intensity and low background of atomic or ionic emission lines in LIBS spectra.

Delay time optimization experiments were carried out under the same focusing distance (17.5cm), spot size (100 μ m), laser pulse duration time (10 ns), gate time (100 μ s) and constant laser pulse energy (100 mJ). Therefore, experiments were

performed to optimize the detector delay time (t_d) with a minimum deviation in the experimental parameters.

Figure 4.3. shows signal intensity variation of Pt (I) lines with respect to detector delay time. At late delay times, signal intensity usually decreases however a substantial decrease in background emission increases the S/N ratio of the measurements. At early delay times a high background emission decreases the S/N ratio. Therefore, neither too early nor too late detector delay times are suitable for high signal to noise ratio in LIBS measurements.

A detector delay time of 2200 ns has been chosen as optimum delay time (t_d) for the rest of the measurements to obtain the highest signal intensity.

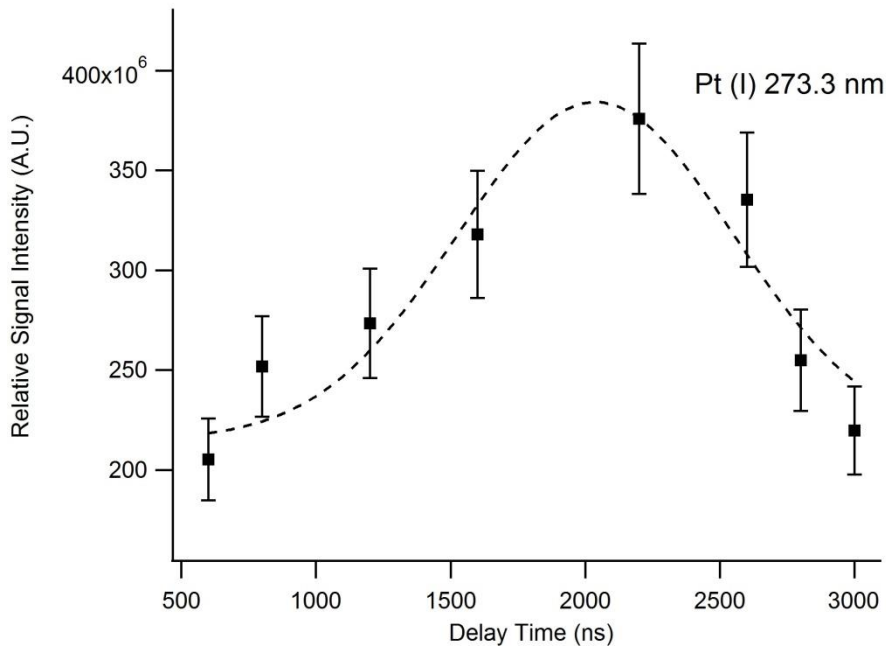


Figure 4.3. LIBS signal intensity variation of Pt (I) at 273.3 nm with respect to detector delay time (Laser pulse energy: 100 mJ, Tg: 100 μ s).

Optimization experiments to determine the optimum detector gate time were also performed on dried polyacrylamide gel. As shown in figure 4.4, relative signal intensity of Pt (I) line at 273.3 nm emission increases up to 200 μ s and then drastically decreases. Therefore, 200 μ s was chosen as the optimum detector gate time and used throughout the experiments.

Unless otherwise noted, all the experiments were performed with optimum instrumental parameters; 100 mJ laser pulse energy, 2200 ns detector delay time (t_d) and 200 μ s detector gate time (t_g).

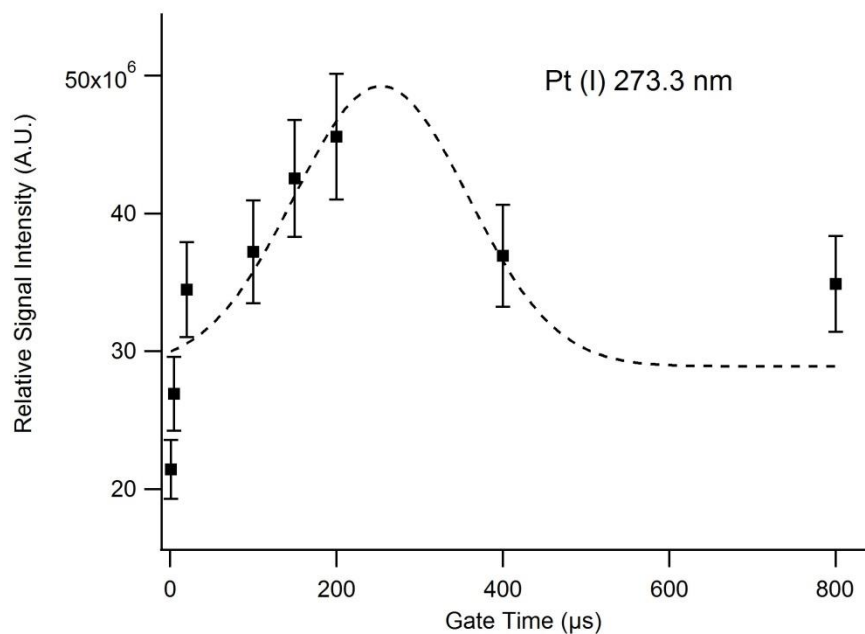


Figure 4.4. LIBS signal intensity variation of Pt (I) at 273.3 nm with respect to detector gate time (Laser pulse energy: 100 mJ, T_d : 1000 ns).

To investigate the lateral variation of Pt (I) lines on the dried polyacrylamide gel samples, Pt (I) at 273.3 nm to C (I) 247.8 nm ratios were calculated for the data obtained from 50 different spots on the dried gel. As can be seen in Figure 4.5, the variation in Pt (I) / C (I) signal is within the normal errors of LIBS measurements with a relative standard deviation of 7.64 % over the entire region on the dried polyacrylamide gel. One can conclude that the distribution of Pt (I) lines at 273.3 nm is quite homogeneous.

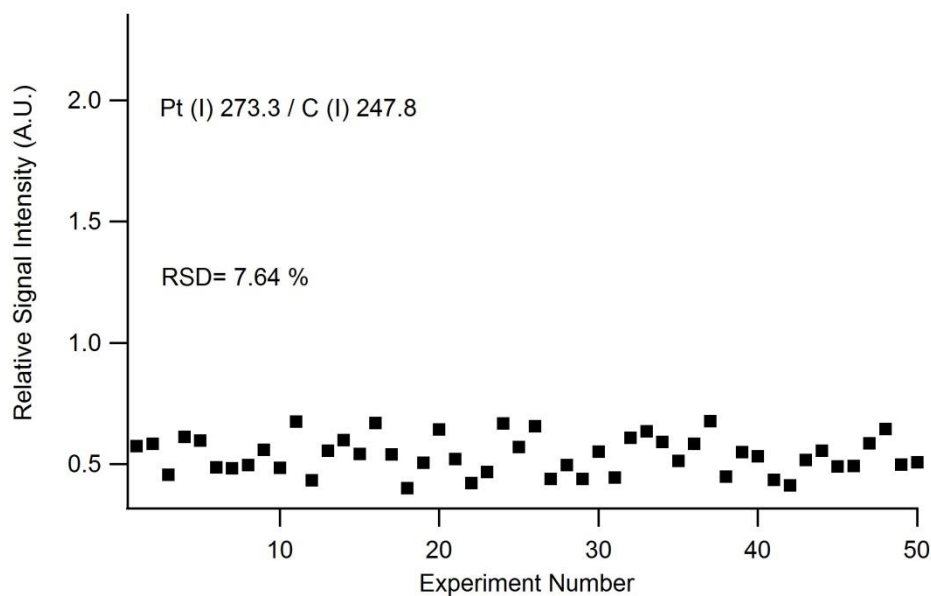


Figure 4.5. Lateral variation of of Pt (I) lines on the dried polyacrylamide gel samples. Laser pulse energy: 100 mJ, $t_d= 2200\text{ns}$, $t_g: 200 \mu\text{s}$. Signals were obtained from 3 consecutive laser shots.

4.2. Verification of Cis-platin-Binding to Proteins by ESI-MS

Verification of cis-platin binding to standard proteins have been performed by ESI-MS prior to nr-SDS-PAGE separation.

Human apo-transferrin (Sigma-Aldrich T1147), human serum albumin (Sigma-Aldrich A3782) and myoglobin from equine heart (Sigma-Aldrich M1882), each in 60 μM concentration were separately incubated with cis-platin solution at a molar ratio of 1:40 in a buffer containing NaCl (4.64 mM) and Tris-NO₃ (10 mM, pH 7.4). Then, these solutions were incubated for 24h at 37 °C in a thermostatic bath (JP Selecta 7471200). All the solutions were diluted to 5 μM concentration before ESI-MS analysis and cis-platin binding to proteins were monitored for 24 hours. Control samples were also prepared by incubating the same proteins under the same conditions without cisplatin solution.

ESI-MS spectra of myoglobin protein incubated with and without cisplatin solution at different incubation times within 24 hours are given in Figure 4.6 and Figure 4.7, respectively.

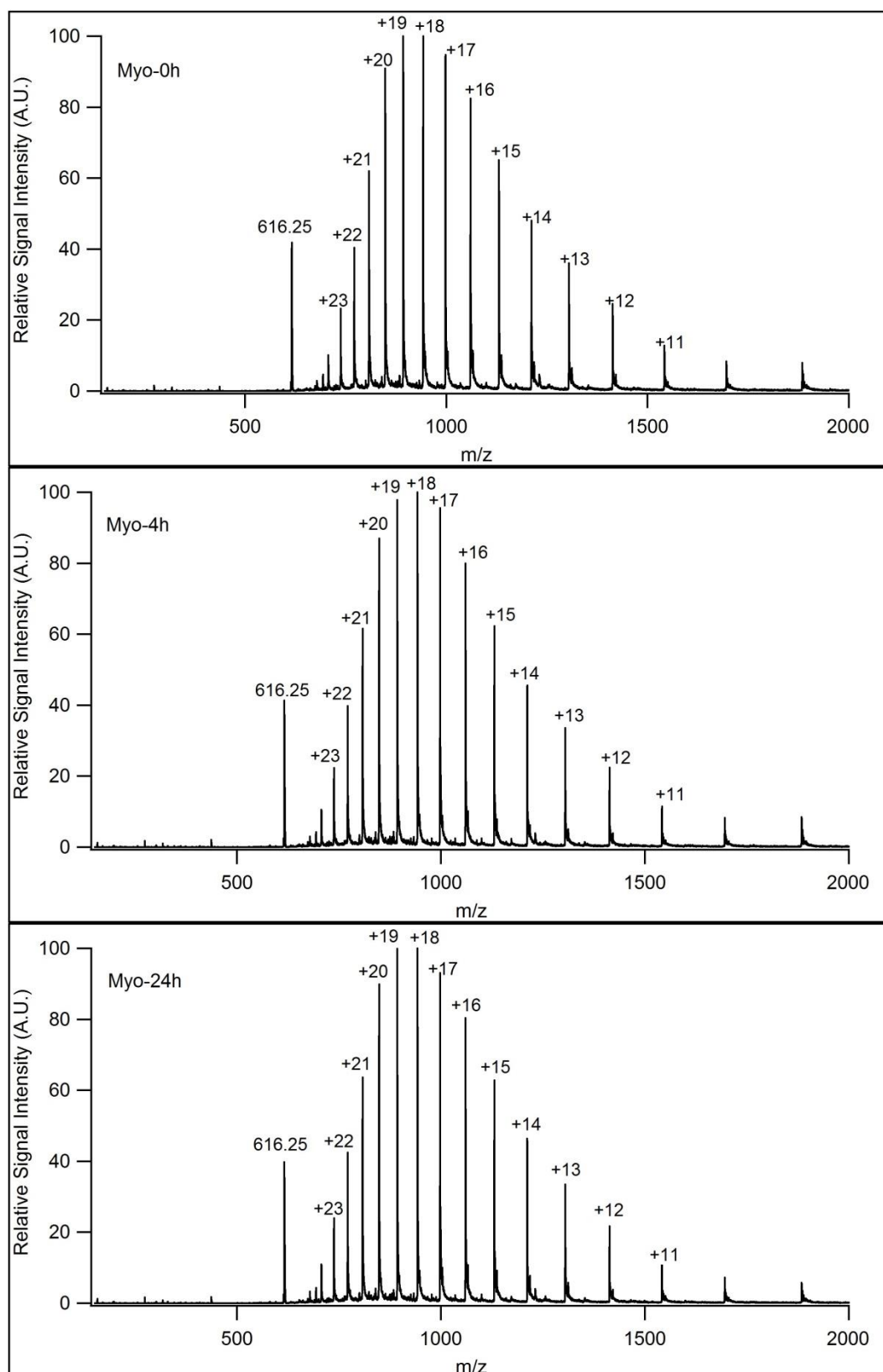


Figure 4.6. ESI-MS spectra of myoglobin incubated during 24 h in physiological buffer solution at 37 °C.

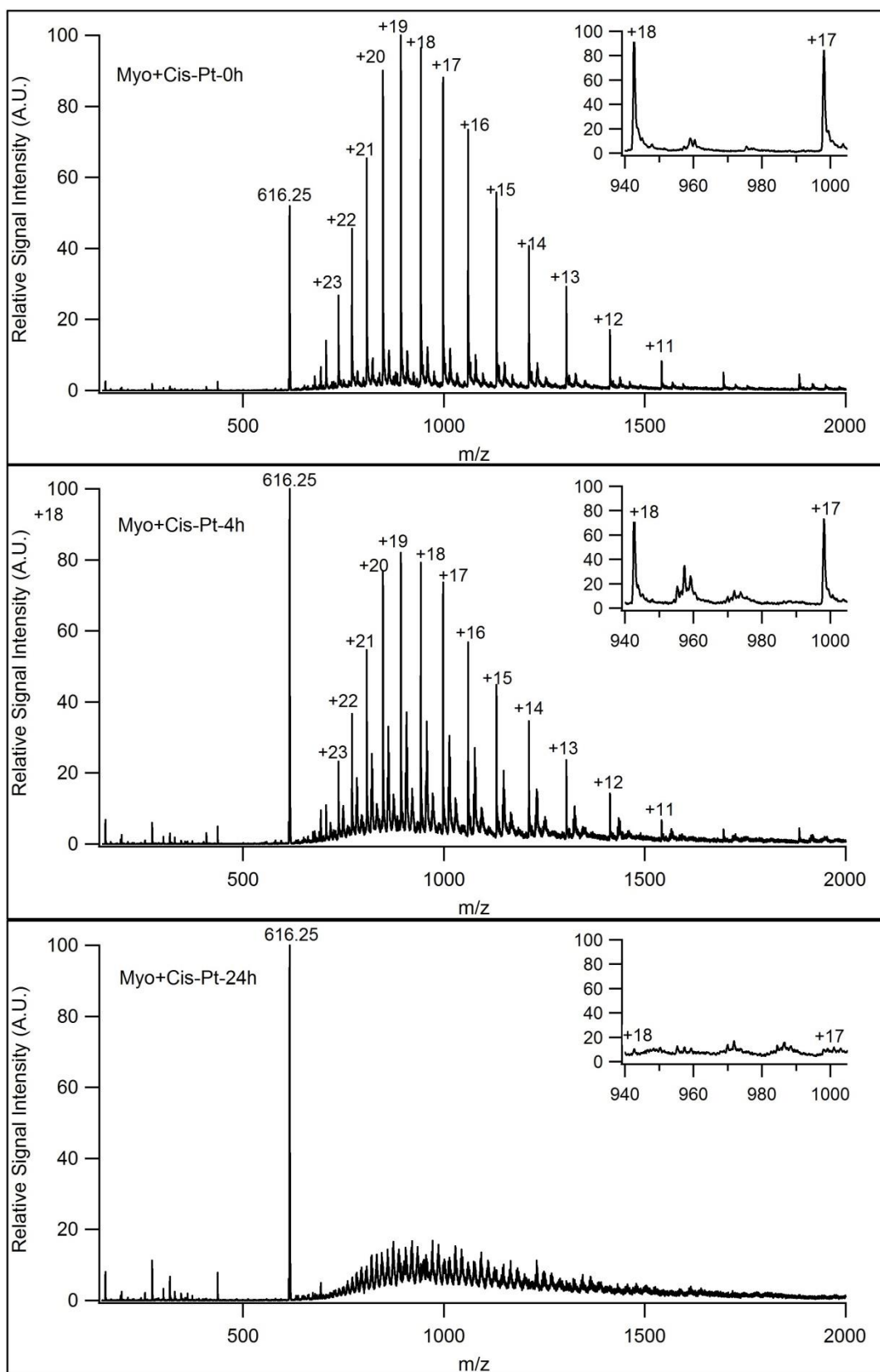


Figure 4.7. ESI-MS spectra of myoglobin incubated with cis-platin solution during 24 h in physiological buffer solution at 37 °C.

As can be seen in Figure 4.6, there is no significant change in myoglobin's spectra taken at different incubation times, indicating no degradation of myoglobin in physiological buffer solution during 24 h incubation time, at 37 °C. However, there are dramatic differences in the spectra of myoglobin incubated with cis-platin solution, as is given in Figure 4.7. In both spectra, the peak at 616.25 (m/z) belongs to the porphyrin ring with an iron at the center of myoglobin's structure. Other peaks represent multiply charged ions of myoglobin molecule. Insets in each spectra time evolution of myoglobin-cisplatin adducts is given for clarity.

Myoglobin and cis-platin adduct ions have also been observed in the ESI-MS spectra. It can be concluded that adduct formation starts just after mixing the solutions and increases as the reaction time proceeds. It is assumed that many different conformations of cis-platin can make an adduct with myoglobin molecule from its nucleophilic sides. Therefore, as the reaction proceeds different peaks of adduct ion formation was observed.

For bigger proteins, adduct formation assumed to be faster due to more number of nucleophilic sides available on their structure. Figure 4.8 shows ESI-MS spectra of human serum albumin protein during 24 h incubation without cisplatin solution. HSA shows no degradation in physiological buffer solution after 24 h incubation at 37 °C.

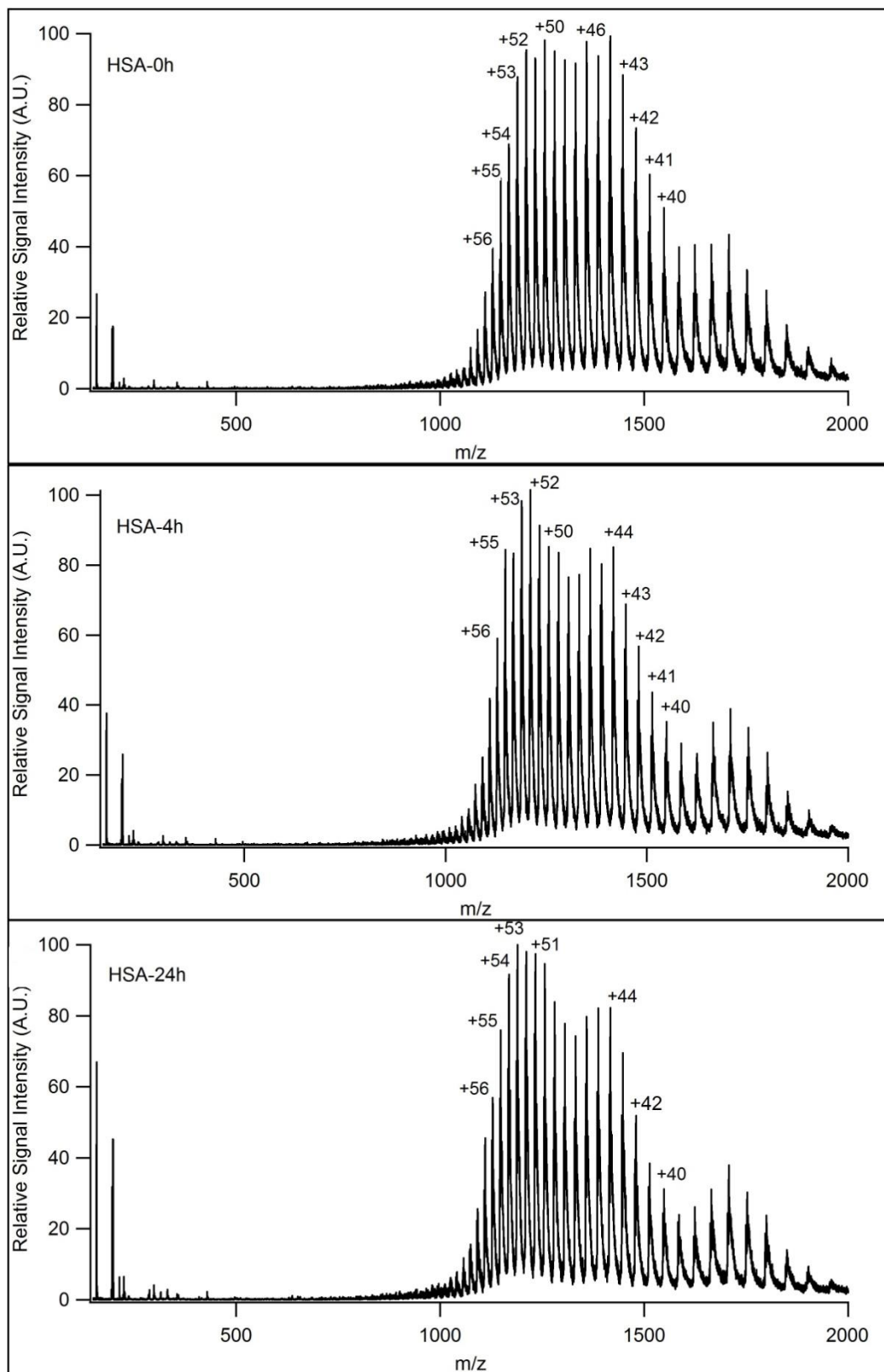


Figure 4.8. ESI-MS spectra of HSA during 24 h incubation in physiological buffer solution at 37 °C.

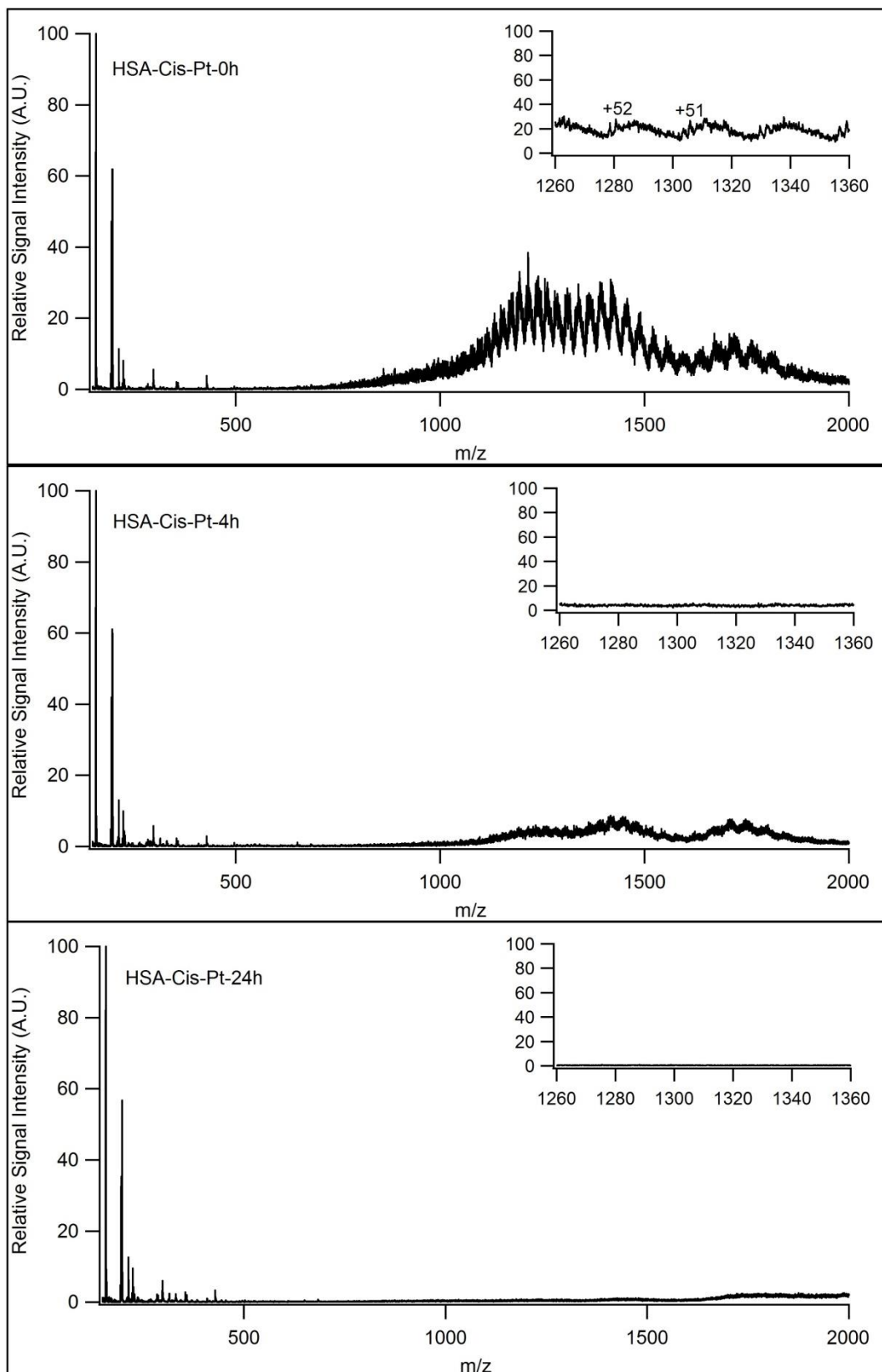


Figure 4.9. ESI-MS spectra of HSA incubated with cis-platin solution during 24 h in physiological buffer solution at 37 °C.

As shown in figure 4.9, HSA binds to cis-platin much faster than myoglobin. This is due to the presence of more nucleophilic sides available on HSA's molecular structure. Compared to the myoglobin, large number of adduct formation occurs in a shorter time and multiply charged ion peaks decreases much more faster in HSA than in myoglobin.

Due to the limitations in the spectral range of the instrument, LTQ XL linear ion-trap mass spectrometer (Thermo Finnigan, San Jose, CA, USA), multiply charged ions of human apo-transferrin could not be observed.

4.3. Separation of Cisplatin Binding Protein by nr-SDS-PAGE

Denaturing chemicals used in sodium dodecyl sulfate polyacrylamide gel electrophoresis (SDS-PAGE) can result in metaldrug-protein bond lose. Therefore, non-reducing sodium dodecyl sulfate polyacrylamide gel electrophoresis (nr-SDS-PAGE) in which the protein-metaldrug adduct structure protected, was used for electrophoretic separation of cis-platin-binding proteins. For this purpose, separated proteins were stained by Coomassie Brilliant Blue staining technique. Stained gels were destained and mounted in between two hydrophobic membranes (Gel air Drying System, Bio-Rad™) and left for drying at room temperature prior to LIBS analysis. After drying specific regions of interest were cut and placed on 3-D translational stage prior to LIBS analysis.

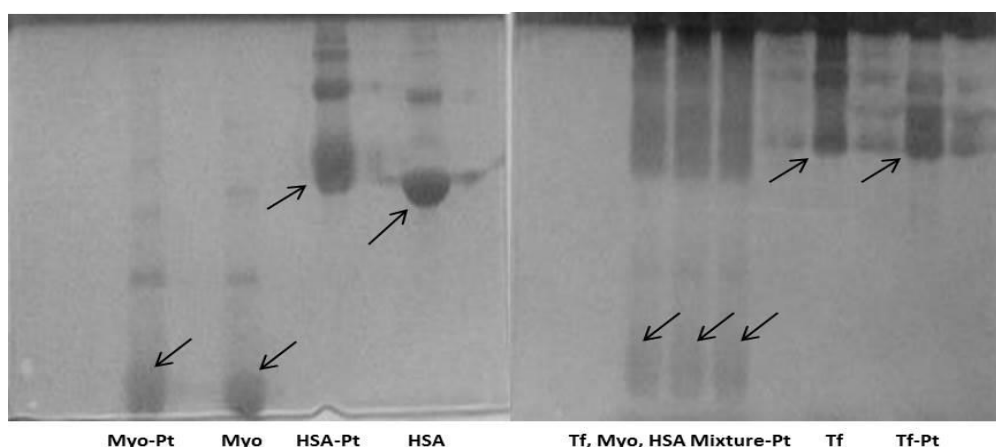


Figure 4.10. nr-SDS-PAGE separation of individual standard proteins incubated with cis-platin. The main bands representing the standard proteins are indicated by arrows.

Polymerization of protein molecules due to the complexation with cis-platin have been observed in all standard protein samples after incubation for 96 h. Separation of HSA, Tf and Myo mixture incubated with cis-platin was not well resolved on the polyacrylamide gel. This can be related to complexation of cis-platin with more than one different protein molecules in the mixture.

4.4. Morphology of Laser Ablated Craters on Gel

Laser ablated craters on the gels were investigated through scanning electron microscopy pictures. Figure 4.11, from top to bottom, shows the SEM (Philips XL30 Environmental SEM FEG) pictures of craters obtained from single and 2, 3, 4, 5 laser shots each with 100 mJ of laser pulse energy.

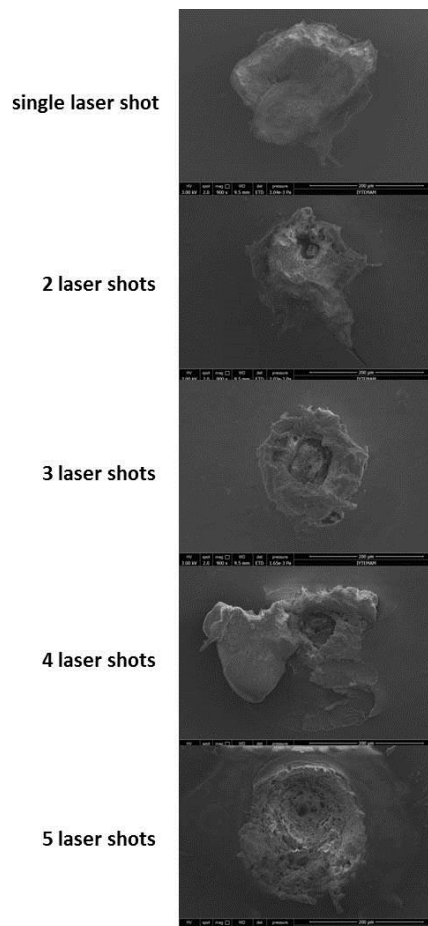


Figure 4.11. SEM images of spots after 5 consecutive laser shots on dried polyacrylamide gels in between the hydrophobic membranes (laser pulse energy: 100 mJ, t_d : 2200 ns, t_g : 200 μ s).

The first laser shot cannot reach the gel in between the membranes. The second laser shot totally removes the surface of the hydrophobic membrane. After the third shot, laser pulse reaches the gel and we start to observe Pt (I) emission lines at 273.3 nm. We could not observe Pt (I) signals after the fifth laser shot.

4.5. LIBS Analysis of Cis-platin Binding Proteins in Gel

Polyacrylamide gels dried in between the two hydrophobic membranes were analyzed in order to determine the platinum content of nr-SDS-PAGE separated proteins. Samples were subjected to consecutive laser shots under optimum instrumental conditions (laser pulse energy: 100 mJ, t_d : 2200 ns, t_g : 200 μ s).

Figure 4.12 shows the five consecutive LIBS spectra of HSA on dry polyacrylamide gels. In general, all the spectra are dominated by strong hydrogen, oxygen, nitrogen, calcium and sodium lines. These are common elements to proteins and buffer solutions used in sample preparation stages. Pt (I) line at 273.3 nm could not be observed until the third shot due to the presence of cellophane sheet in front of the gel. The ablation depth of the first laser shot is not enough to reach the gel in between the membranes therefore only in the third shot Pt (I) emission line at 273.3 nm starts to be observed. Also, Pt (I) emission could not be observed after the fifth laser shot, in most of the measurements, due to around 1 mm thickness of the gel. Insets in each spectra enlarged view of the spectral region between 272-275 nm were presented for clarity.

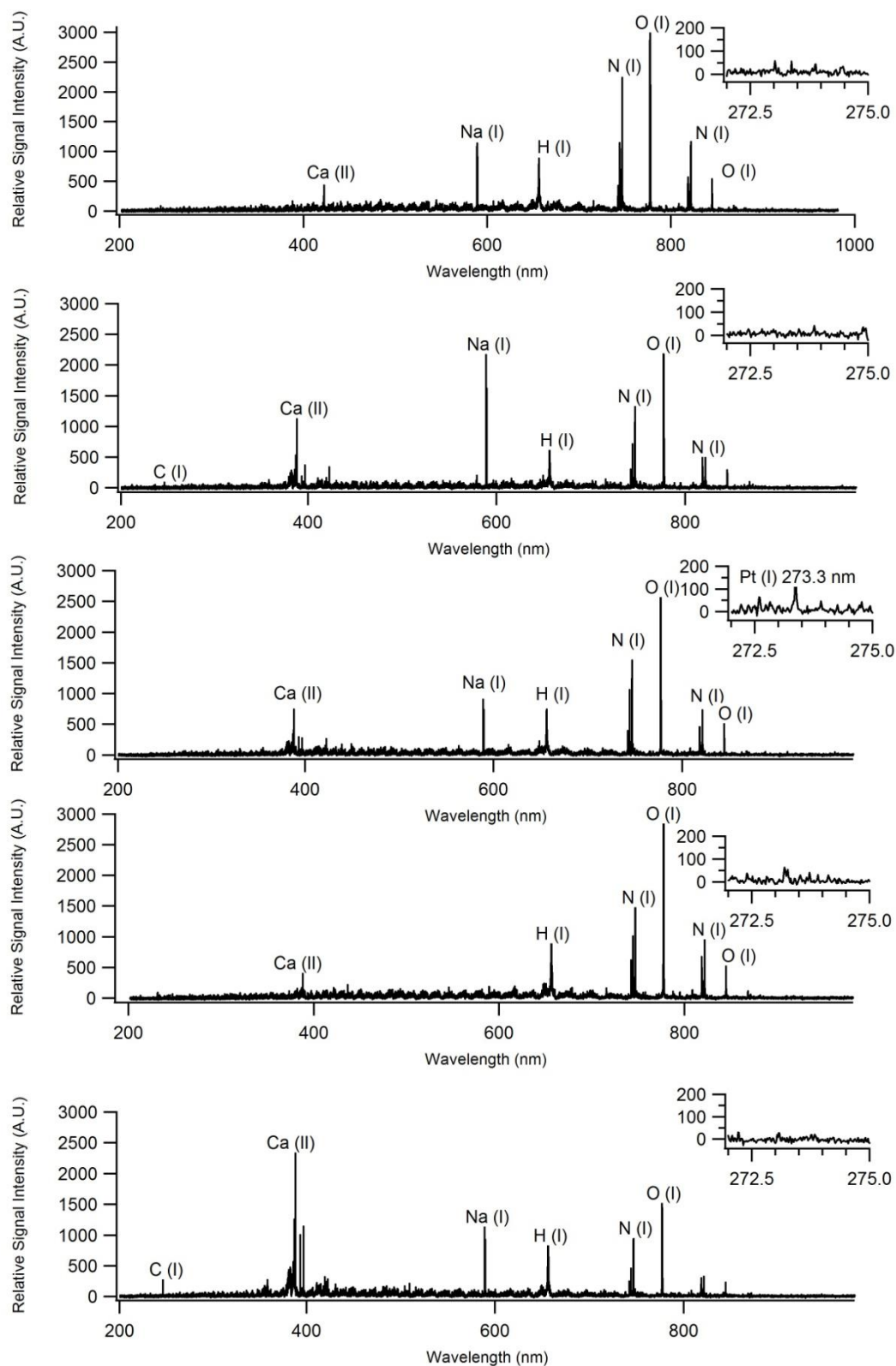


Figure 4.12. Representative LIBS spectra of HSA on dried polyacrylamide gels in between the hydrophobic membranes which were obtained from five consecutive laser shots (laser pulse energy: 100 mJ, t_d : 2200 ns, t_g : 200 μ s).

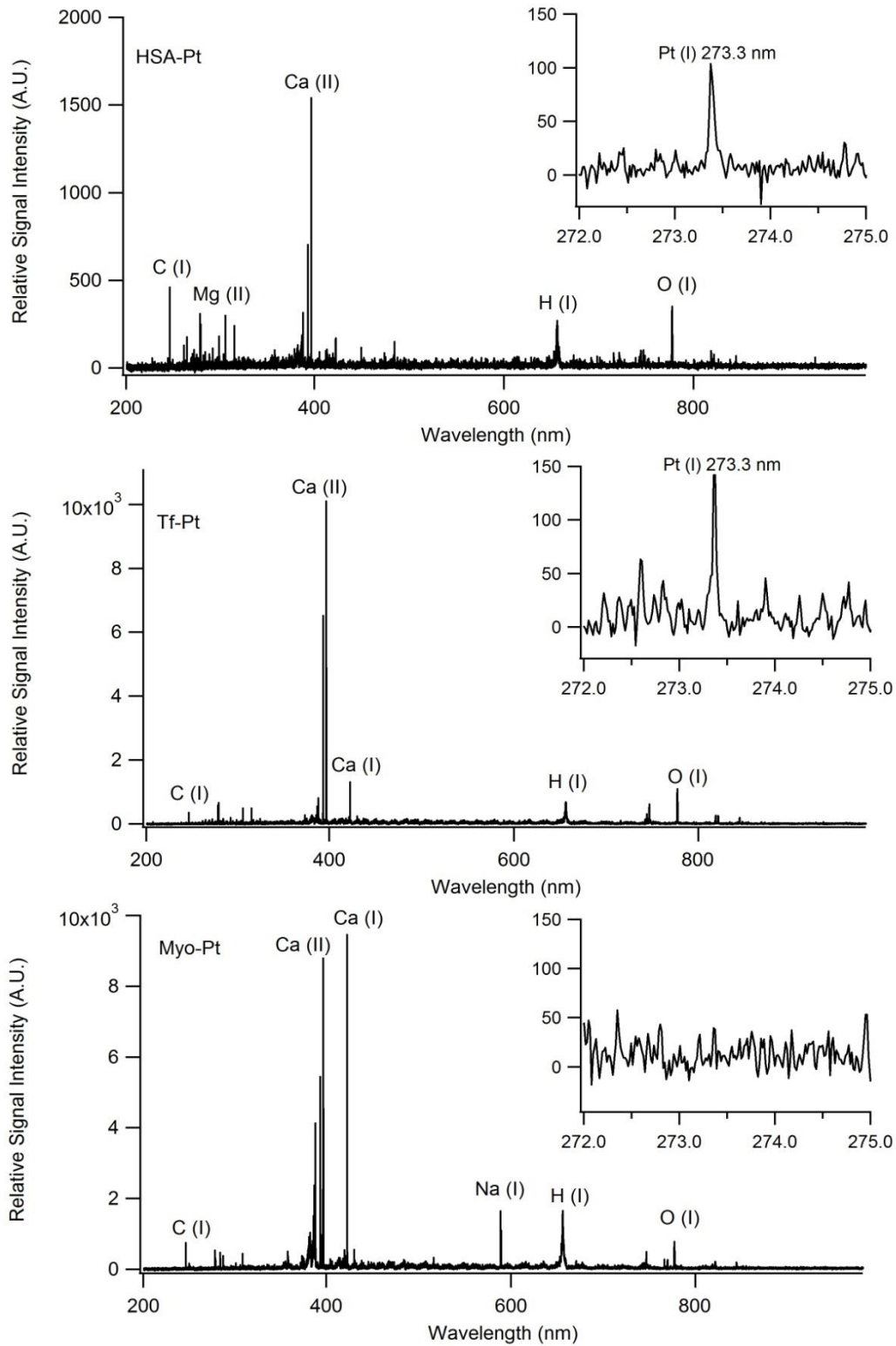


Figure 4.13. Qualitative analysis of HSA-Pt, Tf-Pt and Myo-Pt on dried polyacrylamide gels in between hydrophobic membranes after separation (laser pulse energy: 100 mJ, t_d : 2200 ns, t_g : 200 μ s).

After LIBS analysis on dried polyacrylamide gels, we observed Pt (I) emission lines at 273.3 nm for HSA and Tf whereas we could not observe any Pt (I) emission for Myo as shown in figure 4.13. Myoglobin is relatively a smaller molecule than HSA and Tf. Therefore, its nucleophilic binding sites are less in number than HSA's and Tf's nucleophilic sites. Since, myoglobin binds less amount of cis-platin molecule we could not observe any Pt (I) lines on the spectra.

4.6. In Vitro Investigations of Protein Extracts from Cancer Line

Total proteins from human cervical cancer cells (HeLa cells) were extracted and analyzed with our method. Firstly, we have applied SDS-PAGE and nr-SDS-PAGE separation of total protein extracts to observe the presence of proteins in cancer cells.

Figure 4.14 shows both nr-SDS-PAGE and SDS-PAGE separation of protein extracts from human cervical cancer cells. As we can observe SDS-PAGE separation provides better resolution of the proteins compared to nr-SDS-PAGE. This is because of the fact that denaturing chemicals used in SDS-PAGE provides a single polypeptide chain of the proteins, whereas nr-SDS-PAGE preserves quaternary, tertiary and secondary structure of the protein which results in broadening of the protein band in the gel. From the nr-SDS-PAGE, one can conclude that there are four different protein bands in between 25-116 kDa separated in the gel.

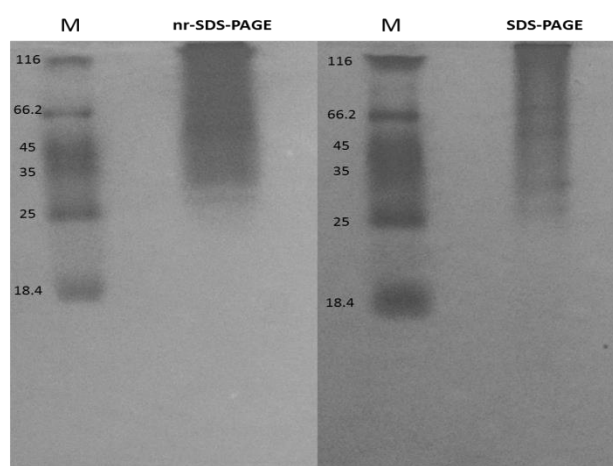


Figure 4.14. nr-SDS-PAGE and SDS-PAGE patterns of protein extracts from human cervical cancer cells. M: protein molecular weight marker.

Total protein solutions were treated with a concentrated cisplatin and nr-SDS-PAGE separation performed prior to LIBS analysis. Figure 4.15 shows nr-SDS-PAGE separation of protein extracts and standard HSA protein treated with cis-platin. Entire region of proteins from extracts on the gel and HSA-Pt spots were mounted in between two hydrophobic membranes, dried and analyzed by LIBS. We observed Pt (I) emission lines at 273.3 nm for HSA-Pt complex whereas we could not observe any signal from the entire region of protein extracts. We can conclude that detection limit of LIBS is not enough to utilize our method for the detection of Pt content in protein spots on the gel for total protein solutions. This is due to the low concentrations of proteins in real samples which increases the limit of detection.

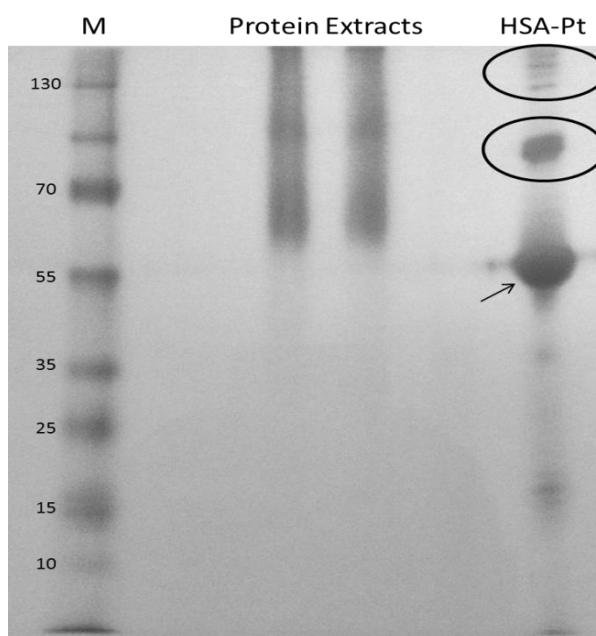


Figure 4.15. nr-SDS-PAGE gel showing separation of protein extracts from human cervical cancer cells and HSA incubated with cisplatin, along with the protein molecular weight markers (M). HSA-Pt complex indicated by arrow. Bands showing the polymerization of HSA indicated in circles.

Representative LIBS spectra of HSA-Pt complex and protein extracts were shown in figure 4.16. Insets in each spectra enlarged view of the spectral region between 272-275 nm were presented for clarity.

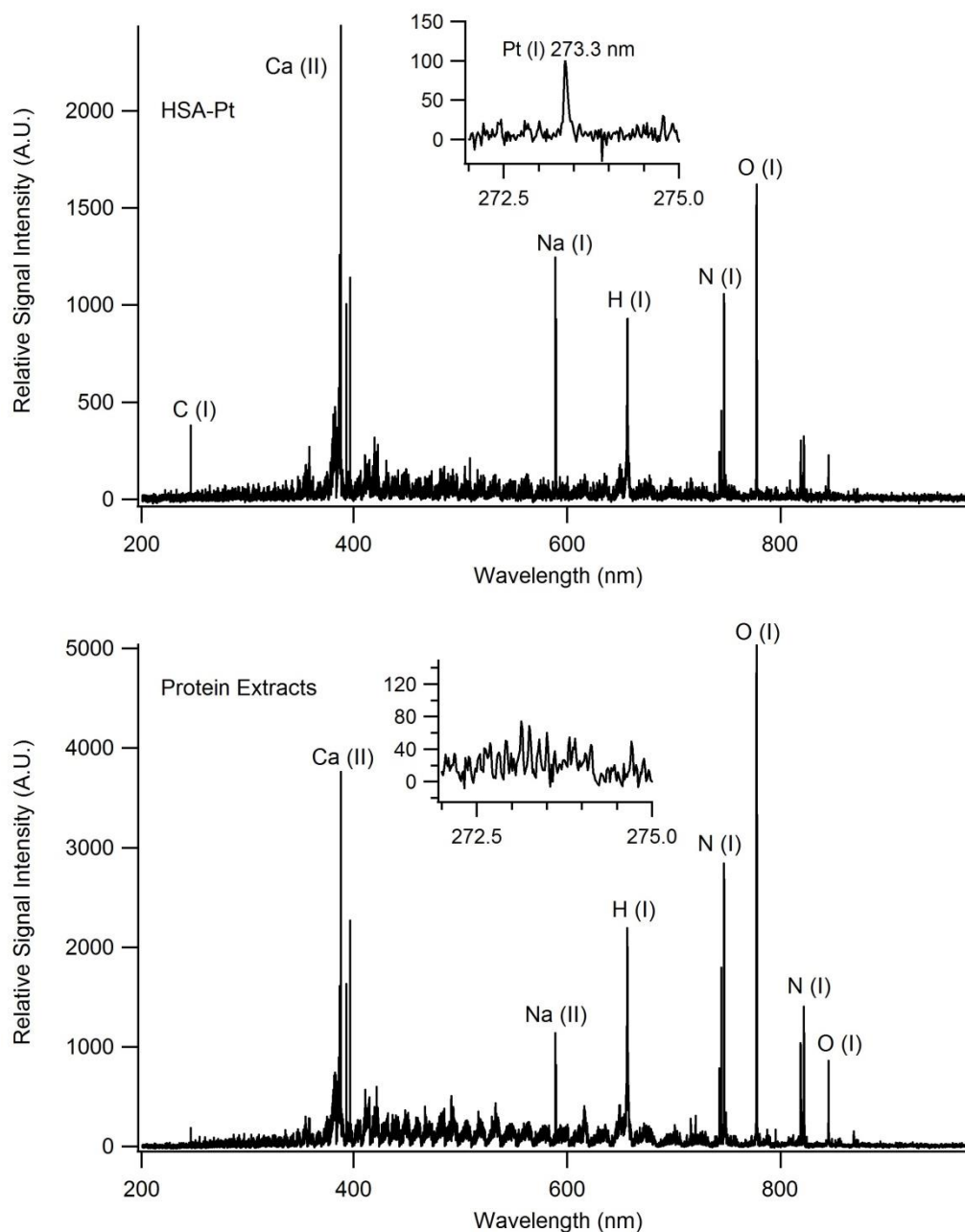


Figure 4.16. Representative LIBS spectra of HSA-Pt complex and protein extracts (laser pulse energy: 100 mJ, t_d : 2200 ns, t_g : 200 μ s).

To utilize our method in vitro conditions, we added different concentrations of HSA solutions to the total protein solutions extracted from HeLa cancer cells, separated by nr-SDS-PAGE and analyzed by LIBS. Figure 4.17 shows nr-SDS-PAGE separations of HSA-added total protein solutions. Due to the high detection limits of LIBS we have added concentrated solutions of HSA into the total protein solutions.

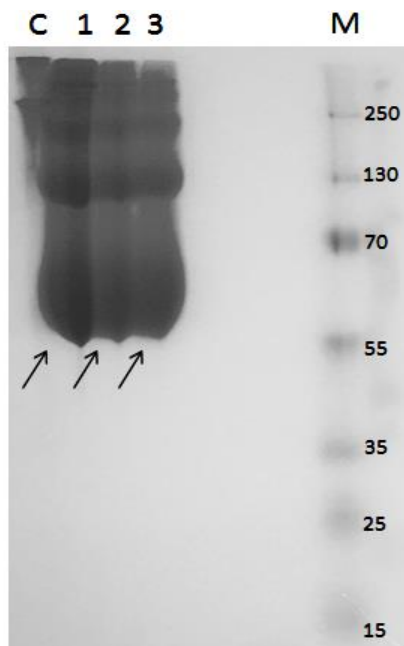


Figure 4.17. nr-SDS-PAGE gel showing separation of protein extracts added HSA. M: molecular weight marker, C: protein extract without HSA, and 1,2,3 represents concentration gradient of protein extracts added HSA. HSA-Pt complexes indicated by arrows.

All the region over the gel were analyzed by LIBS for platinum content. Pt (I) emission signals at 273.3 nm were observed for HSA-Pt complexes 1 and 2, whereas no signal observed for control and 3. We can conclude that LIBS can be useful to determine Pt (I) contents of HSA-Pt complexes in vitro conditions with a nanogram level of detection. However, our detection limit may not be sufficient for real samples due to the low concentrations of analytes.

CHAPTER 5

CONCLUSIONS

In this study, an all-optically designed laser plasma spectroscopic technique for rapid identification and detection of cisplatin-binding proteins on electrophoretic gel spots prior to molecular mass spectrometric analysis for proteome research is demonstrated. Non-reducing polyacrylamide gel electrophoretic separation followed by the visualization of proteins in the gel by Coomassie Brilliant Blue staining technique was applied. Protein spots on the gel were dried between two cellophane sheets and subjected to laser ablation by highly energetic laser pulses. In addition, prior to nr-SDS-PAGE separation cis-platin binding to standard proteins were monitored by ESI-MS with several measurements made in 24 hours of incubation time.

LIBS emission signals were observed for Pt-HSA and Pt-Apo-transferrin complex however, no signal from the Pt-Myo complex has been observed after electrophoretic separation. It has been demonstrated that, LIBS is a suitable method for identifying Pt in proteins, in gel medium, with nanogram to picogram levels of detection capability.

The technique was utilized to identify the Pt signals in HSA-Pt complex after electrophoretically separated proteins from HSA-added HeLa cells (human cervical cancer cells) extract with a nanogram level detection limit.

LIBS is a simple, rapid and sensitive optical spectroscopic technique which requires no sample preparation for the identification of Pt-binding proteins on electrophoretic gel spots prior to molecular mass spectrometric analysis.

REFERENCES

- Adis, R, and D Profile. 2007. "BMS 182751, BMY 45594, JM 216."
- Allardyce, Claire S, Paul J Dyson, Fadi R Abou-Shakra, Heather Birtwistle, and Jonathan Coffey. 2001. "Inductively coupled plasma mass spectrometry to identify protein drug targets from whole cell systems." *Chemical Communications* (24):2708-2709.
- Aras, Nadir, and Şerife Yalçın. 2014. "Rapid identification of phosphorus containing proteins in electrophoresis gel spots by Laser-Induced Breakdown Spectroscopy, LIBS." *Journal of Analytical Atomic Spectrometry* 29 (3):545-552.
- Bordui, Peter F, and Martin M Fejer. 1993. "Inorganic crystals for nonlinear optical frequency conversion." *Annual Review of Materials Science* 23 (1):321-379.
- Capitelli, F, F Colao, MR Provenzano, R Fantoni, G Brunetti, and N Senesi. 2002. "Determination of heavy metals in soils by laser induced breakdown spectroscopy." *Geoderma* 106 (1):45-62.
- Chan, SY, and NH Cheung. 2000. "Analysis of solids by laser ablation and resonance-enhanced laser-induced plasma spectroscopy." *Analytical chemistry* 72 (9):2087-2092.
- Chrambach, A, RA Reisfeld, Mr Wyckoff, and J Zaccari. 1967. "A procedure for rapid and sensitive staining of protein fractionated by polyacrylamide gel electrophoresis." *Analytical biochemistry* 20 (1):150-154.
- Cremers, DA, JE Barefield, and AC Koskelo. 1995. "Remote elemental analysis by laser-induced breakdown spectroscopy using a fiber-optic cable." *Applied Spectroscopy* 49 (6):857-860.
- Cremers, David A, and Leon J Radziemski. 1985. "Direct detection of beryllium on filters using the laser spark." *Applied spectroscopy* 39 (1):57-63.
- Cremers, David A, Fang-Yu Yueh, Jagdish P Singh, and Hansheng Zhang. 2006. *Laser-Induced Breakdown Spectroscopy, Elemental Analysis*: Wiley Online Library.
- Cui, Meng, and Zoltan Mester. 2003. "Electrospray ionization mass spectrometry coupled to liquid chromatography for detection of cisplatin and its hydrated complexes." *Rapid communications in mass spectrometry* 17 (14):1517-1527.
- De Giacomo, A, M Dell'Aglio, F Colao, R Fantoni, and V Lazic. 2005. "Double-pulse LIBS in bulk water and on submerged bronze samples." *Applied surface science* 247 (1):157-162.

- DeLucia Jr, Frank C, Alan C Samuels, Russell S Harmon, Roy Walters, Kevin L McNesby, Aaron LaPointe, Raymond J Winkel Jr, and Andrzej W Miziolek. 2005. "Laser-induced breakdown spectroscopy (LIBS): a promising versatile chemical sensor technology for hazardous material detection." *Sensors Journal, IEEE* 5 (4):681-689.
- Diedrich, Jonathan, Steven J Rehse, and Sunil Palchadhuri. 2007. "Escherichia coli identification and strain discrimination using nanosecond laser-induced breakdown spectroscopy." *Applied Physics Letters* 90 (16):163901.
- El-Hussein, A, AK Kassem, H Ismail, and MA Harith. 2010. "Exploiting LIBS as a spectrochemical analytical technique in diagnosis of some types of human malignancies." *Talanta* 82 (2):495-501.
- Esteban-Fernandez, D, JM Verdaguer, R Ramirez-Camacho, MA Palacios, and MM Gomez-Gomez. 2008. "Accumulation, fractionation, and analysis of platinum in toxicologically affected tissues after cisplatin, oxaliplatin, and carboplatin administration." *Journal of analytical toxicology* 32 (2):140-146.
- Esteban-Fernández, Diego, María Montes-Bayón, E Blanco González, MM Gomez Gomez, MA Palacios, and Alfredo Sanz-Medel. 2008. "Atomic (HPLC-ICP-MS) and molecular mass spectrometry (ESI-Q-TOF) to study cis-platin interactions with serum proteins." *Journal of Analytical Atomic Spectrometry* 23 (3):378-384.
- Esteban-Fernández, Diego, Estefanía Moreno-Gordaliza, Benito Cañas, María Antonia Palacios, and María Milagros Gómez-Gómez. 2010. "Analytical methodologies for metallomics studies of antitumor Pt-containing drugs." *Metallomics* 2 (1):19-38.
- Gaona, I, P Lucena, J Moros, FJ Fortes, S Guirado, J Serrano, and JJ Laserna. 2013. "Evaluating the use of standoff LIBS in architectural heritage: surveying the Cathedral of Málaga." *Journal of Analytical Atomic Spectrometry* 28 (6):810-820.
- Giakoumaki, Anastasia, Kristalia Melessanaki, and Demetrios Anglos. 2007. "Laser-induced breakdown spectroscopy (LIBS) in archaeological science—applications and prospects." *Analytical and bioanalytical chemistry* 387 (3):749-760.
- Griem, Hans R. 1963. "Validity of local thermal equilibrium in plasma spectroscopy." *Physical review* 131 (3):1170.
- Griem, Hans R. 2005. *Principles of plasma spectroscopy*. Vol. 2: Cambridge University Press.
- Harmon, Russell S, Frank C DeLucia, Catherine E McManus, Nancy J McMillan, Thomas F Jenkins, Marianne E Walsh, and Andrzej Miziolek. 2006. "Laser-induced breakdown spectroscopy—An emerging chemical sensor technology for

- real-time field-portable, geochemical, mineralogical, and environmental applications." *Applied geochemistry* 21 (5):730-747.
- Haruna, Masamitsu, Masato Ohmi, Mitsuo Nakamura, and Shigeto Morimoto. 2000. "Calcium detection of human hair and nail by the nanosecond time-gated spectroscopy of laser-ablation plume." *BiOS 2000 The International Symposium on Biomedical Optics*.
- Jodrell, Duncan I, Merrill J Egorin, Renzo M Canetta, Patricia Langenberg, Ellie P Goldbloom, James N Burroughs, Janis L Goodlow, Sylvia Tan, and Eve Wiltshaw. 1992. "Relationships between carboplatin exposure and tumor response and toxicity in patients with ovarian cancer." *Journal of clinical oncology* 10 (4):520-528.
- Kaiser, Jozef, Michaela Galiová, Karel Novotný, Rostislav Červenka, Lucia Reale, Jan Novotný, Miroslav Liška, Ota Samek, Viktor Kanický, and Aleš Hrdlička. 2009. "Mapping of lead, magnesium and copper accumulation in plant tissues by laser-induced breakdown spectroscopy and laser-ablation inductively coupled plasma mass spectrometry." *Spectrochimica Acta Part B: Atomic Spectroscopy* 64 (1):67-73.
- Kiss, ZJ, and RJ Pressley. 1966. "Crystalline solid lasers." *Applied optics* 5 (10):1474-1486.
- Kondo, A, M Maeta, A Oka, S Tsujitani, M Ikeguchi, and N Kaibara. 1996. "Hypotonic intraperitoneal cisplatin chemotherapy for peritoneal carcinomatosis in mice." *British journal of cancer* 73 (10):1166.
- Kumar, Akshaya, Fang-Yu Yueh, Jagdish P Singh, and Shane Burgess. 2004. "Characterization of malignant tissue cells by laser-induced breakdown spectroscopy." *Applied optics* 43 (28):5399-5403.
- Laemmli, Ulrich K. 1970. "Cleavage of structural proteins during the assembly of the head of bacteriophage T4." *nature* 227 (5259):680-685.
- Laville, Stéphane, Christian Goueguel, Hakim Loudyi, François Vidal, Mohamed Chaker, and Mohamad Sabsabi. 2009. "Laser-induced fluorescence detection of lead atoms in a laser-induced plasma: An experimental analytical optimization study." *Spectrochimica Acta Part B: Atomic Spectroscopy* 64 (4):347-353.
- Manzoor, S, S Moncayo, F Navarro-Villoslada, JA Ayala, R Izquierdo-Hornillos, FJ Manuel de Villena, and JO Caceres. 2014. "Rapid identification and discrimination of bacterial strains by laser induced breakdown spectroscopy and neural networks." *Talanta* 121:65-70.
- Markushin, Yuri, Poopalasingam Sivakumar, Denise Connolly, and Nouredine Melikechi. 2015. "Tag-femtosecond laser-induced breakdown spectroscopy for the sensitive detection of cancer antigen 125 in blood plasma." *Analytical and bioanalytical chemistry* 407 (7):1849-1855.

- McColm, AA, A McLaren, G Klinkert, MR Francis, PC Connolly, CJ Grinham, CJ Campbell, S Selway, and R Williamson. 1996. "Ranitidine bismuth citrate: a novel anti-ulcer agent with different physico-chemical characteristics and improved biological activity to a bismuth citrate-ranitidine admixture." *Alimentary pharmacology & therapeutics* 10 (3):241-250.
- Mena, M^a Luz, Estefanía Moreno-Gordaliza, Irene Moraleja, Benito Cañas, and M^a Milagros Gómez-Gómez. 2011. "OFFGEL isoelectric focusing and polyacrylamide gel electrophoresis separation of platinum-binding proteins." *Journal of Chromatography A* 1218 (9):1281-1290.
- Miziolek, Andrzej W, Vincenzo Palleschi, and Israel Schechter. 2006. *Laser induced breakdown spectroscopy*: Cambridge University Press.
- Moreno-Gordaliza, Estefanía, Diego Esteban-Fernández, Charlotte Giesen, Karola Lehmann, Alberto Lázaro, Alberto Tejedor, Christian Scheler, Benito Cañas, Norbert Jakubowski, and Michael W Linscheid. 2012. "LA-ICP-MS and nHPLC-ESI-LTQ-FT-MS/MS for the analysis of cisplatin–protein complexes separated by two dimensional gel electrophoresis in biological samples." *Journal of Analytical Atomic Spectrometry* 27 (9):1474-1483.
- Nygren, Olle, Gary T Vaughan, T Mark Florence, Gregory MP Morrison, Ian M Warner, and Leslie S Dale. 1990. "Determination of platinum in blood by adsorptive voltammetry." *Analytical chemistry* 62 (15):1637-1640.
- Pera, MF, and Harold C Harder. 1977. "Analysis for platinum in biological material by flameless atomic absorption spectrometry." *Clinical chemistry* 23 (7):1245-1249.
- Pinto, Ann L, and Stephen J Lippard. 1985. "Binding of the antitumor drug cis-diamminedichloroplatinum (II)(cisplatin) to DNA." *Biochimica et Biophysica Acta (BBA)-Reviews on Cancer* 780 (3):167-180.
- Raab, Andrea, Barbara Pioselli, Caroline Munro, Jane Thomas-Oates, and Jörg Feldmann. 2009. "Evaluation of gel electrophoresis conditions for the separation of metal-tagged proteins with subsequent laser ablation ICP-MS detection." *Electrophoresis* 30 (2):303-314.
- Rehse, Steven J, Jonathan Diedrich, and Sunil Palchaudhuri. 2007. "Identification and discrimination of *Pseudomonas aeruginosa* bacteria grown in blood and bile by laser-induced breakdown spectroscopy." *Spectrochimica Acta Part B: Atomic Spectroscopy* 62 (10):1169-1176.
- Rosenberg, Barnett, Loretta Van Camp, and Thomas Krigas. 1965. "Inhibition of cell division in *Escherichia coli* by electrolysis products from a platinum electrode." *Nature* 205 (4972):698-699.
- Russo, Richard E, Xianglei Mao, and Samuel S Mao. 2002. "Peer reviewed: The physics of laser ablation in microchemical analysis." *Analytical chemistry* 74 (3):70 A-77 A.

- Sallé, Béatrice, David A Cremers, Sylvestre Maurice, and Roger C Wiens. 2005. "Laser-induced breakdown spectroscopy for space exploration applications: Influence of the ambient pressure on the calibration curves prepared from soil and clay samples." *Spectrochimica Acta Part B: Atomic Spectroscopy* 60 (4):479-490.
- Samek, O, DCS Beddows, HH Telle, J Kaiser, M Liška, JO Caceres, and A Gonzales Urena. 2001. "Quantitative laser-induced breakdown spectroscopy analysis of calcified tissue samples." *Spectrochimica Acta Part B: Atomic Spectroscopy* 56 (6):865-875.
- Samek, Ota, Jorg Lambert, R Hergenröder, Miroslav Liška, Jozef Kaiser, Karel Novotný, and Sergei Kukhlevsky. 2006. "Femtosecond laser spectrochemical analysis of plant samples." *Laser Physics Letters* 3 (1):21-25.
- Samuels, Alan C, Frank C DeLucia, Kevin L McNesby, and Andrzej W Miziolek. 2003. "Laser-induced breakdown spectroscopy of bacterial spores, molds, pollens, and protein: initial studies of discrimination potential." *Applied optics* 42 (30):6205-6209.
- Sancey, L, V Motto-Ros, B Busser, S Kotb, JM Benoit, A Piednoir, F Lux, O Tillement, G Panczer, and J Yu. 2014. "Laser spectrometry for multi-elemental imaging of biological tissues." *Scientific reports* 4.
- Shevchenko, Andrej, Henrik Tomas, Jan Havli, Jesper V Olsen, and Matthias Mann. 2006. "In-gel digestion for mass spectrometric characterization of proteins and proteomes." *Nature protocols* 1 (6):2856-2860.
- Singh, Jagdish P, and Surya Narayan Thakur. 2007. *Laser-induced breakdown spectroscopy*: Elsevier.
- Singh, Vivek K, Vinay Kumar, and Jitendra Sharma. 2014. "Importance of laser-induced breakdown spectroscopy for hard tissues (bone, teeth) and other calcified tissue materials." *Lasers in medical science*:1-16.
- Singh, Vivek K, and Awadhesh K Rai. 2011. "Potential of laser-induced breakdown spectroscopy for the rapid identification of carious teeth." *Lasers in medical science* 26 (3):307-315.
- St-Onge, Louis, Elizabeth Kwong, Mohamad Sabsabi, and EB Vadas. 2002. "Quantitative analysis of pharmaceutical products by laser-induced breakdown spectroscopy." *Spectrochimica Acta Part B: Atomic Spectroscopy* 57 (7):1131-1140.
- Summons, Roger E, Jan P Amend, David Bish, Roger Buick, George D Cody, David J Des Marais, Gilles Dromart, Jennifer L Eigenbrode, Andrew H Knoll, and Dawn Y Sumner. 2011. "Preservation of martian organic and environmental records: final report of the Mars Biosignature Working Group." *Astrobiology* 11 (2):157-181.

- Sun, Qing, Michael Tran, Benjamin W Smith, and James D Winefordner. 2000. "Zinc analysis in human skin by laser induced-breakdown spectroscopy." *Talanta* 52 (2):293-300.
- Sun, Xuesong, Cheuk-Nam Tsang, and Hongzhe Sun. 2009. "Identification and characterization of metallodrug binding proteins by (metallo) proteomics." *Metallomics* 1 (1):25-31.
- Sutton, Blaine M, Elizabeth McGusty, Donald T Walz, and Michael J DiMartino. 1972. "Oral gold. Antiarthritic properties of alkylphosphinegold coordination complexes." *Journal of medicinal chemistry* 15 (11):1095-1098.
- Tesniere, A, F Schlemmer, V Boige, O Kepp, I Martins, F Ghiringhelli, L Aymeric, M Michaud, L Apetoh, and L Barault. 2010. "Immunogenic death of colon cancer cells treated with oxaliplatin." *Oncogene* 29 (4):482-491.
- Timerbaev, Andrei R, Svetlana S Aleksenko, Kasia Polec-Pawlak, Rafal Ruzik, Olga Semenova, Christian G Hartinger, Slawomir Oszwaldowski, Markus Galanski, Maciej Jarosz, and Bernhard K Keppler. 2004. "Platinum metallodrug-protein binding studies by capillary electrophoresis-inductively coupled plasma-mass spectrometry: Characterization of interactions between Pt (II) complexes and human serum albumin." *Electrophoresis* 25 (13):1988-1995.
- Timerbaev, Andrei R, Christian G Hartinger, Svetlana S Aleksenko, and Bernhard K Keppler. 2006. "Interactions of antitumor metallodrugs with serum proteins: advances in characterization using modern analytical methodology." *Chemical reviews* 106 (6):2224-2248.
- Wang, Xu, Yin Wei, Qingyu Lin, Ji Zhang, and Yixiang Duan. 2015. "A Simple, Fast Matrix Conversion and Membrane Separation Method for Ultrasensitive Metal Detection in Aqueous Samples by Laser Induced Breakdown Spectroscopy." *Analytical chemistry*.
- Wong, Ernest, and Christen M Giandomenico. 1999. "Current status of platinum-based antitumor drugs." *Chemical reviews* 99 (9):2451-2466.
- Yueh, Fang-Yu, Hongbo Zheng, Jagdish P Singh, and Shane Burgess. 2009. "Preliminary evaluation of laser-induced breakdown spectroscopy for tissue classification." *Spectrochimica Acta Part B: Atomic Spectroscopy* 64 (10):1059-1067.